Unexpected high frequency of nocturnal surface ozone enhancement events over China: Characteristics and mechanisms

Cheng He[1,2], Xiao Lu[1,2*], Haolin Wang[1,2], Haichao Wang[1,2], Yan Li[3], Guowen He[1,2], Yuanping He[1,2], Yurun Wang[4], Youlang Zhang[1,2], Yiming Liu[1,2], Qi Fan[1,2], Shaojia Fan[1,2*]

[1]School of Atmospheric Sciences, Sun Yat-sen University, and Key Laboratory of Tropical Atmosphere-Ocean System, Ministry of Education, Zhuhai, China
[2]Guangdong Provincial Observation and Research Station for Climate Environment and Air Quality Change in the Pearl River Estuary, Southern Marine Science and Engineering Guangdong Laboratory (Zhuhai), Zhuhai, China
[3]School of Environmental Science and Engineering, China West Normal University, Nanchong, China
[4]Department of Land, Air, and Water Resources, University of California Davis, Davis, USA

Correspondence to: Xiao Lu (luxiao25@mail.sysu.edu.cn) and Shaojia Fan (eesfsj@mail.sysu.edu.cn)

Abstract. Surface ozone concentrations typically peak in daytime driven by active photochemical production and decrease gradually after sunset by chemical destruction and dry deposition. Here, we report that nocturnal ozone enhancement (NOE, defined as ozone increase by more than~~at least~~ 5 ppbv hour^{-1}~~ ~~ in one of any two adjacent hours in 20:00-06:00 local time) events are observed at multiple monitoring sites in China at a high frequency that has not been recognized in previous studies. We present an overview of the general characteristics of NOE events in China and explore the possible mechanisms based on six-year observations from the national monitoring network. We find that the ~~annual~~ mean annual frequency of NOE events is 41±10% (i.e. about 140 days would experience NOE event per year) averaged over all 814 Chinese sites in 2014-2019, which is 46% larger than those over Europe and US. The NOE event frequency is higher in industrialized city clusters (>50%) than regions with lighter ozone pollution, and is higher in the warm (46%) than cold season (36%), consistent with the spatiotemporal evolution of ozone levels. The mean ozone peak during NOE events reaches 37±6 ppbv in the warm season. The ozone enhancements are within 5-15 ppbv hour^{-1} in 85% of the NOE events, but in about 10% of the cases the ozone increases can exceed 20 ppbv hour^{-1}. ~~ ~~We propose that the high photochemistry-induced ozone in the daytime provides rich ozone source in the nighttime residual layer, determining the overall high frequency of NOE events in China, and then the enhanced atmospheric mixing triggers NOE events by allowing the ozone-rich air in the residual layer to mix into the nighttime boundary layer. This is supported by our analyses that 70% (65%) of the NOE events are associated with increases in friction velocity (planetary boundary layer height), indicative of enhanced atmospheric mixing, and also supported by the observed sharp decreases in surface NO_2 and CO concentrations with ozone increases in NOE events, a typical signal of mixing with air in the residual layer. Three case studies in Beijing and Guangzhou show~~s~~ that synoptic processes such as convective storms and low-level jets can lead to the NOE event by aggravating vertical mixing. Horizontal transport of ozone-rich plumes may also be a supplementary driver of NOE event. Our results summarize for the first time the characteristics and mechanism of the NOE events in China based on nationwide and long-term observations, and call for more direct measurements and modeling studies on the nighttime ozone evolution from surface to the residual layer.

1 Introduction

Surface-layer ozone is a major air pollutant and controls the oxidation capacity of the atmospheric boundary layer. Ozone is mainly generated from the sunlight-driven photochemical reactions of nitrogen oxides (NO_x, $NO \pm NO_2$), carbon monoxide (CO), and volatile organic compounds (VOCs) that released from anthropogenic and natural sources at the surface (Sillman, 1995; Jacob, 2000; Monks et al., 2015). It is also transported downward from the upper troposphere or even stratosphere with mesoscale dynamic processes triggering deep stratospheric incursions (Stohl et al., 2003; Škerlak et al., 2014; Wang et al., 2020). Surface-layer ozone levels in polluted regions typically increase in daytime fostered by photochemical formation in the presence of solar radiation and emissions of precursors, and decrease gradually after sunset by chemical destruction (i.e. NO_x titration) and dry deposition, shaping the well-established single daytime peak pattern of ozone diurnal cycle (Lin et al., 2008; Strode et al., 2019). Here, we report that nocturnal ozone enhancement events are observed at multiple monitoring sites in China at a high frequency that have not been recognized in previous studies.

Analyses of the nocturnal ozone enhancement events and associated ~~nighttime~~ ozone peaks have important implications for ~~human health, vegetation growth, and~~ nocturnal atmospheric dynamics and chemistry, as well as ozone exposure to human and vegetation health. Due to the lack of nighttime chemical source, elevated nocturnal ozone levels are thought to be driven by enhanced transport or atmospheric mixing, which can be indicative of atmospheric dynamic processes such as the boundary-layer low-level jets (Klein et al., 2014). The enhanced nighttime ozone then reshapes the ozone diurnal cycle, and may increase daily integrated ozone exposure time to human and vegetation that threatens human health. ~~Ozone toxicity is capable of stimulating the lining of the lung and other surfaces in the respiratory tract and thus increases both short-term and long-term risks of respiratory and circulatory mortality~~ (Turner et al., 2016; Fleming et al., 2018) and crop yields. ~~With rapid urbanization and the consequent increasing numbers of population travelling and working nighttime, exposure to enhanced nocturnal ozone levels may increase the threats of cardiovascular and respiratory diseases. Surface ozone is also harmful to vegetation growth and crop yields through damaging plant leaf cells~~ (Yue et al., 2017; Lefohn et al., 2018; Feng et al., 2022; Li et al., 2022). Enhanced nocturnal ozone can also increase the oxidation capacity by simulating the nitrate radical formation (Wang et al., 2021), and promote the formation of secondary pollutants such as particulate nitrate and secondary organic aerosols (Brown and Stutz, 2012; Huang et al., 2020). It can further affect atmospheric chemistry of the following day ~~Although ozone-induced damages to vegetation are most prominent at daytime due to more vigorous metabolic activities and higher ozone concentrations, nighttime ozone also impairs stomatal function of plants such as tobacco which is more active at night (De Moraes et al., 2001; Cordeiro et al., 2021). Meanwhile, elevated nocturnal ozone may enhance the oxidation capacity that promotes the formation of secondary pollutants and affect atmospheric chemistry of the following day~~ (Millet et al., 2016; Caputi et al., 2019; Zhao et al., 2020). While long-term trends of mean nighttime ozone level have been extensively studied as an important metric for assessing ozone air quality and emission changes (Cooper et al., 2012;

Lu et al., 2020), the more episodic nocturnal ozone enhancement event has been underappreciated despite its unusuality and important implication.

A number of studies have reported episodic nocturnal ozone enhancement events at individual sites around the world (Eliasson et al., 2003; Hu et al., 2012; Hu et al., 2013; Klein et al., 2014; Kulkarni et al., 2016; Caputi et al., 2019; Zhu et al., 2020; He et al., 2021).The reported nocturnal ozone enhancement were mostly ranging from 5 to 30 ppbv, but can be up to 70 ppbv in an extreme event observed in summer 2013 over the North China Plain (Jia et al., 2015). The mean nocturnal ozone peaks during these episodes may exceed 40 ppbv (Zhu et al., 2020), sufficiently high to threat human and vegetation health. Previous studies have identified that horizontal transport of ozone-rich air from polluted regions, and enhanced turbulence and vertical mixing which can be triggered by synoptic processes such as convective storms and low-level jets, are the mechanisms for driving the nocturnal ozone enhancement (Reitebuch et al., 2000; Hu et al., 2013; Klein et al., 2014; Caputi et al., 2019). These studies, however, focused on episodic cases at only one or a few sites and were limited to timescales of days or months. A comprehensive view on the general characteristics and mechanisms of the nocturnal ozone enhancements based on multi-year and large-scale observation monitoring network is missing.

In this study, we examine the frequency, peak ozone values, magnitude, and trend of the nocturnal ozone enhancement (NOE) events over China, based on six -years (2014-2019) of ozone observations from the nationwide monitoring network. We compare the frequency of NOE events in China with that in the United States and Europe in the same period to demonstrate the higher frequency of NOE events over China than the other two regions which has not been recognized in previous studies. We then explore the potential drivers of the NOE events over China, by examining the evolution of nighttime chemical components and meteorological factors indicative of atmospheric mixing ability in the NOE events. Our study provides the first overview of the nocturnal ozone enhancement events in China, which adds new insights to surface ozone evolution and may have important implications for designing ozone regulation strategies.

2 Data and methodology

2.1 Surface observations of ozone and air pollutants over China, Europe, and the United States

The nationwide hourly observations of surface air pollutants (ozone, NO_2, and CO) in mainland China are obtained from the China National Environmental Monitoring Center (CNEMC) network (http://106.37.208.233:20035/, last access: 15 April 2022). The network was initiated from 2013 at 74 key cities for air pollution monitoring, and expanded rapidly to more than 400 cities afterwards (Figure S1). The dataset has been applied in many studies for analyzing the diurnal cycle, season shifts, and interannual variations of ozone levels over Chinese cities (Wang et al., 2017b; Guo et al., 2019; Liu and Wang, 2020; Lu et al., 2020; Li et al., 2021). Here we use the hourly data from 2014 to 2019 at 814 sites covering 74 cities with continuous ozone observations in the six-year period (Figure S1). The measurements are reported at Beijing time (UTC +8) in unit of μg

m^{-3}, and we transfer them to mixing ratios (ppbv) at local time (LT) based on the time zone of sites. We carry out data quality controls for observations of all pollutants to remove potential data outliers following (Lu et al., 2018) and (Jiang et al., 2021) (Supplementary information).

We use additionally hourly surface ozone observations from the United States (US) and Europe (EU) in the same 2014-2019 period for a global comparison of the frequency of nocturnal ozone enhancement events. Ozone observations at 762 sites over US and 1880 sites over EU (Fig.S1) are obtained from the US Environmental Protection Agency (https://aqs.epa.gov/aqsweb/airdata/download_files.html, last access: 15 April 2022) and the European Environment Agency (https://discomap.eea.europa.eu/Index/, last access: 15 April 2022), respectively. We also convert the measurements to local time in unit of ppbv and apply the same data quality control procedures to these observations as to the CNMEC observations.

2.2 Meteorological parameters and ozone from the ERA5 dataset

We apply three-dimensional fields of meteorological parameters including temperature, relative humidity, horizontal and vertical wind speed and direction on pressure levels, and two-dimensional fields of planetary boundary layer height, and friction velocity from the ERA5 dataset, i.e. the fifth generation of the European Centre for Medium-Range Weather Forecasts (ECMWF) atmospheric reanalysis of the global climate (https://cds.climate.copernicus.eu/#!/home, last access: 15 April 2022). The ERA5 dataset combines observations of meteorological parameters across the world with model outputs, and has been extensively evaluated with independent observations of key meteorological parameters in the troposphere (Hersbach et al., 2020). The three-dimensional ozone fields from the ERA5 dataset are also utilized for the analysis of ozone vertical transport. We use the ERA5 data with the horizontal resolution at 0.25°×0.25°, vertical resolution of 25 hPa, and temporal resolution at 1 hour. We sample the ERA5 data at the grid of a monitoring site for site-level analyses.

2.3 Definition of nocturnal ozone enhancement event and related magnitude and nocturnal ozone peaks

Following previous studies of Eliasson et al. (2003) and Zhu et al. (2020) We define the period of 20:00 (LT) to 06:00 (LT) of the next day as the nighttime period. Following previous studies of (Eliasson et al., 2003; Zhu et al., 2020), we define a nocturnal ozone enhancement (NOE) event if ozone concentration at a site increases by more than 5 ppbv ($\Delta O_3/\Delta t > 5\ ppb\ hour^{-1}$) in one of any two adjacent hours in the nighttime period. We find that nocturnal $\Delta O_3/\Delta t$ values at Chinese sites generally follow the Gaussian distribution, and $\Delta O_3/\Delta t > 5\ ppb\ hour^{-1}$ cases only account for 7.7% of the $\Delta O_3/\Delta t$ dataset, indicating that this definition should have effectively ruled out nocturnal ozone fluctuations occur under normal atmospheric conditions (Fig. S2). We only define one NOE event if there are more than one hour with ($\Delta O_3/\Delta t > 5\ ppb\ hour^{-1}$) at a specific night, and observations with the maximum $\Delta O_3/\Delta t$ are used for statistical analyses. We also define the corresponding magnitude of an NOE event as the maximum of ozone enhancement in the two adjacent hours in the nighttime period (maximum of $\Delta O_3/\Delta t$). The nocturnal ozone peak in an NOE event is defined as the maximum of ozone concentrations in the nighttime period. For comparison, we define a non-enhanced non-nocturnal ozone enhancement

4

130 (NNOE) event if the maximum of ozone change in all adjacent two hours in the nighttime period is less than 1 ppbv (maximum of $\Delta O_3/\Delta t < 1\ ppb\ hour^{-1}$).

3 Results and discussion

3.1 Frequency and magnitude of NOE events from 2014 to 2019

Figure 1a compares the annual frequency of the NOE events over China, Europe, and the continental US averaged over
135 2014-2019. We estimate the frequency of NOE events of 41±10% (mean ± standard deviation, 814 sites) averaged for all Chinese sites in 2014-2019, with 140 sites showing a frequency of 50% or higher. The annual frequency of NOE events over China are 46% larger than those over Europe (28±12%, 1880 sites) and US (28±13%, 762 sites), and this high frequency of NOE events is largely unrecognized among current ozone studies in China. Spatially, sites with high frequency of NOE events (>50%) are widely distributed across the industrialized regions such as the North China Plain (NCP), Yangtze River
140 Delta (YRD), Pearl River Delta (PRD), and Sichuan Basin (SCB), and also scattered at regions of western China, Mediterranean, and western US. These regions have been previously identified as hotspots of severe surface ozone pollution due to either high anthropogenic emissions of ozone precursors or natural background ozone (Zhang et al., 2014; Wang et al., 2017a; Lu et al., 2018; Lu et al., 2021). As shown in Fig.1b and 1c, the spatial pattern of NOE event frequencies is closely related to the afternoon (14-17 LT) ozone and nighttime O_x (O_3+NO_2) concentrations measured at the surface. This feature
145 has important implications for understanding the mechanism of NOE events, which will be analyzed in Section 3.2. As will be discussed later, the spatial pattern of NOE event frequencies is closely related to the afternoon (14-17 LT) ozone concentrations measured at the surface as shown in Figure 1b.

Figure 2 compares the frequency and nocturnal ozone peak of NOE events in the warm (April-September) and cold (other
150 months) season across the Chinese monitoring sites. We see notable seasonal shifts in the spatial distributions of NOE event frequencies, from 46 ± 11% averaged for all sites in the warm season to 36 ± 10% in the cold season. Regionally, the frequencies of NOE events are higher in the NCP during the warm season, while in the PRD region the frequencies are higher in the cold season (largely driven by October), though there are also large variabilities even at adjacent sites. Sites at western China typically show high frequencies of NOE events throughout the year. These seasonal shifts in the NOE event
155 frequency at different regions are also consistent with the seasonal evolution of ozone concentrations. Previous studies have documented the warm-season peak of ozone over the North China driven by active photochemical formation of ozone in the presence of intensive anthropogenic emissions, and the autumn peak of ozone over the PRD due to the influences of summer monsoon (Lu et al., 2018; Gao et al., 2020). We do not find consistent trends of the NOE frequency across the cities either in the warm or cold season in 2014-2019 (Figure S2).

160

5

We then examine the peak ozone concentrations in the NOE events in Figure 2 to quantify the influences of NOE events on nighttime ozone levels. The NOE-induced nocturnal ozone peaks are 37±6 ppbv and 31±6 ppbv averaged in the warm and cold season, respectively, significantly higher than those in the NNOE events of 17±11 ppbv and 10± 9 ppbv. High nocturnal peak ozone concentrations of more than 50 ppbv in the NOE events are found over the NCP in the warm season. These ozone values can reach over 80% of the corresponding daytime mean ozone concentrations, and are sufficiently high compared to the threshold above which ozone exposures are expected to exert negative effect on human health and vegetation growth (Lefohn et al., 2018). The mean nighttime peak ozone concentration in the NOE events in Beijing is 40 ppbv in the warm season averaged over 2014 to 2019, comparable with Zhu et al. (2020) who found 68.1 μ g m^{-3} (approximately 34 ppbv) averaged in May-September from 2014 to 2015. We also find that at more than 70% sites the peak ozone concentrations in the NOE events show positive trends from 2014-2019 (Figure S3). This may also reflect the rapid increasing nighttime ozone levels in China in this period as reported in Lu et al. (2020).

Figure 3 presents the magnitude of the NOE events (i.e. the maximum of $\Delta O_3/\Delta t$ in the NOE events) over China in the warm season, quantifying the extent of ozone increases in the two adjacent hours during NOE events. We focus on the warm season here because it shows significantly higher frequency of NOE events in most regions (Figure 2). We find that about 85% of the maximum ozone enhancement during NOE events are within 5-15 ppbv hour^{-1}, but in about 10% of the NOE events ozone enhancement can exceed 20 ppbv hour^{-1} within one hour that may significantly change the ozone diurnal cycle. The frequency of small ozone enhancement in the range of 5 to 10 ppb hour^{-1} during NOE events is higher in the southern than in the northern of China, but the pattern reverses for large NOE magnitude exceeding 10 ppb hour^{-1}, reflecting that NOE events may have larger influences on ozone diurnal cycle in the northern China (Figure 3). We also find a significant positive correlation between NOE frequency and magnitude across 814 Chinses sites (r=0.4, p-value<0.01), indicating that sites with more frequent NOE events are more likely to experience larger nighttime ozone increase.

Figure 4 shows the time distribution of NOE events (i.e. the hour when the maximal $\Delta O_3/\Delta t$ occurs) in the five key cities (Beijing, Shanghai, Guangzhou, Chengdu, and Urumqi) representative for different regions in China (Figure 2a), and compares the time series of ozone, NO$_2$, and CO in the NOE events versus the NNOE events. Each city contains a number of monitoring sites, and we average the data across the sites within the city to represent ozone at the city level. We identify 211-419 NOE events for the five cities in the warm season during the 2014-2019 period, corresponding to the frequency of 19%-38%, and 66-314 NNOE events corresponding to the frequency of 6%-29%. The estimated NOE frequency at city level based on the site-average ozone values is lower than that at site level as the occurrence time of NOE events may vary at different sites.

We find that the timing of the NOE event occurrence shows different patterns at these five cities, however, all cities consistently show a small fractions of NOE event occurrence at early night (20:00-21:00 LT). This is reasonable because the

decreasing rate of ozone is fast at early night, due to the rapid chemical loss through NO_x titration ($NO+O_3\rightarrow NO_2+O_2$, $NO_2+O_3\rightarrow NO_3+O_2$, $NO_3+NO_2+M\rightarrow N_2O_5+M$) when emissions are still active and NO levels are high, as evident by the sharp increase in NO_2 with ozone decreases in early night. The ozone decreasing rate (and also NO_2 increasing rate) then slows down with reduced NO levels. In Beijing, the timing of NOE events is diversely evenly distributed across 0:00-6:00 LT with a frequency ranging from 18%-29%, resulting in a flat ozone change when averaging the ozone time series in all NOE events (Figure 4a). In Shanghai, Guangzhou, Chengdu, and Urumqi, a slightly larger fraction of NOE events is occurring at 0:00-3:00 LT, shaping the peak ozone values at around 3:00 LT on average, but in general the timings of NOE events are widely distributed over night (Figure 4b, -4e). The wide distribution in the timing of NOE events indicates that NOE events are more likely driven by episodic synoptic process, rather than anthropogenic-driven factors which otherwise should show a clearer temporal pattern.

Figure 4 illustrates that the occurrences of NOE events change the ozone diurnal cycle and lead to a secondary ozone peak at night. It also reveals the distinguished differences in the temporal evolution of NO_2 and CO between the NOE and NNOE events. NO_2 and CO typically shows increases in the early night because of the shrinking planetary boundary layer, continuous nighttime emissions, and titration (for NO_2 only), and peak at most cities at around 22:00 LT. The concentration of both species decreases afterwards, due to the combined effect of chemical destruction ($NO_2+O_3\rightarrow NO_3+O_2$, $NO_3+NO_2+M\rightarrow N_2O_5+M$), mixing, and deposition, though in Shanghai and Guangzhou a midnight peak of CO at around 2:00 LT is observed that may be linked to regional traffic of heavy vehicles. In particular, we find that NO_2 and CO concentrations decrease at a much faster rate from 22:00-5:00 LT during NOE events, compared to those during NNOE events. This feature has important implications for understanding the potential driver of NOE events as will be discussed in Section 3.2.

3.2 Frequent NOE events associated with high ozone in nighttime residual layer and enhanced vertical mixing

Section 3.1 overviews the general characteristics of NOE events over China, including the spatial and seasonal distributions of NOE event frequencies, peak ozone values, and magnitudes, on the basis of six-year nationwide observations. We now examine what factors determine the overall pattern of NOE event frequencies as displayed in Figure 1a, and trigger the occurrence of NOE events to explain the evolution of ozone, NO_2, and CO as shown in Figure 4. Section 3.3 will present typical episodic NOE events as case studies.

The nighttime ozone decreases are due to the combined effect of net chemical loss, as a result of null photochemical ozone production in the absence of sunlight and the ozone depletion by NO_x titration effect, and the continued ozone dry deposition to surface. Reduced ozone loss by weakening the titration effect and deposition can slow down the nighttime ozone decreasing rate but would not increase ozone. Enhancement of nighttime ozone at a given location thus requires external ozone source, either through horizontal transport from adjacent regions with high ozone levels, or through vertical

transport/mixing of ozone-rich air to surface. The sharper decreases of NO_2 and CO concentrations during NOE events than the NNOE events, as shown in Figure 4, suggest that vertical mixing of air above the surface layer with typically low NO_2 and CO levels is a prioritized candidate. This motivates us to examine:

    (1) whether the regions with high frequency of NOE events, as shown in Figure 1a, are associated with high concentration of nighttime ozone at the residual layer (the region remaining between the stable nocturnal boundary layer at surface and the free atmosphere), and

    (2) whether atmospheric mixing is more active in NOE events that allows the mixing of high-concentration ozone in the residual layer to the surface, compared to NNOE events.

However, examining the first factor is particularly challenged by the extreme sparsity of direct ozone measurements of nighttime residual layer.

Here we propose to use surface ozone averaged over the afternoon (14:00-17:00 LT) as an indicator of ozone level in the nighttime residual layer at a given site. This is because under typical fair-weather conditions, surface ozone is expected to be mixed into the well-developed boundary mixing layer by active atmospheric turbulence in the afternoon. With the sunset, the turbulent mixing in the boundary layer weakens in the absence of solar heating, and the consequent radiative cooling of the ground surface throughout the night forms a stable nocturnal boundary layer with a typical depth of 100-500m above the surface. The erstwhile mixing layer from the daytime, overlying the nighttime boundary layer, is known as the residual layer. It serves as a reservoir for ozone where ozone is not effectively titrated and deposited, so that ozone before sunset is largely remained in the nighttime residual layer (Caputi et al., 2019). Using the afternoon ozone to indicate ozone level in the nighttime residual layer neglects the impact of external transport on ozone to the residual layer, so we suggest that this method makes more sense when the analyses are conducted based on the ensemble of six-year observations, and is achievable for assessing ozone in nighttime residual layer at thousands of sites as direct measurement of ozone vertical profile is rather sparse. Similarly ~~-~~we may use the surface nighttime O_x (O_3+NO_2) concentration as an indicator of ozone in the nighttime residual layer (Kleinman et al., 2002; Wang et al., 2018; Tan et al., 2021), assuming that ~~nighttime NO emissions are low and ozone changes due to~~ nighttime titration is much stronger than the effect of deposition and regional transport.

Figures 1b and 1c presents the mean afternoon ozone and nighttime O_x concentrations~~concentrations~~ over China, Europe, and the US. Comparison of Figure 1a and 1b/1c reveals that the spatial pattern of NOE events frequencies ~~and~~, afternoon ozone levels and nighttime Ox level (both indicative of ozone in the nighttime residual level) are ~~closely related over China, Europe, and the US, respectively~~ largely consistent. In particular, sites over China, Mediterranean, and mountainous western US with frequent NOE events recorded are consistently observing high afternoon ozone level or nighttime O_x level. Figure 5 further shows that NOE frequency at Chinese sites increases with rising mean afternoon ozone level or nighttime O_x level, and is 10% (18%) higher when the afternoon ozone level (nighttime O_x level) exceed 50 ppb, compared to when they are

below 30 ppb.s. ~~We also find similar strong correlations between the pattern of nighttime mean O_x level and NOE event frequencies (Figure S4)~~.

High frequency of NOE events (>50%) and nighttime ozone level in the residual layer as indicated by afternoon ozone or nighttime O_x levels (>50 ppbv) are both found in the industrialized regions over China, including the NCP and YRD city clusters. At night, surface ozone is effectively removed by the NO_x titration and dry deposition, and nighttime ozone levels are on averaged 24 ppbv lower than that in the afternoon (Figure ~~1c~~1d). The afternoon vs nighttime ozone difference is even larger (~30 ppbv) over the NCP, YRD, and PRD regions. Large ozone contrast between the nighttime residual layer and the boundary layer is expected as the afternoon ozone can be largely remained in the nighttime residual layer where ozone is not effectively destructed and deposited. This is evident by a number of measurements of nightime vertical ozone profiles indicating large ozone gradient between the surface and 100-300 meters aloft at different regions in China (Chi et al., 2018; Wang et al. 2018; He et al., 2021). The ozone-rich air in the residual layer can be effectively mixed to the ground once atmospheric mixing is triggered or enhanced by synoptic processes. Regions with higher nighttime ozone in the residual layer are more likely to experience surface ozone increase exceeding the threshold of NOE event definition of $\Delta O_3/\Delta t > 5\ ppb\ hour^{-1}$, compared to regions with lower ozone at similar frequency of enhanced nighttime mixing. This explains the observed co-location of high afternoon ozone concentrations (nighttime O_x concentrations) and NOE event frequencies as shown in Figure 1a and 1b (1c). The strong relationship between the two also explains why the seasonal shifts in frequency and magnitude of NOE event are similar to those in ozone pollution level as presented Section 3.1.

We also see equivalent high frequency of NOE events in Mediterranean and western US, with the afternoon ozone levels (~40 ppbv) sufficiently high compared to other sites in the Europe and US but lower compared to those over China. The afternoon vs nighttime ozone contrast over the Mediterranean and western US is much smaller compared to those observed over China. Ozone at the high-elevation sites over the Mediterranean and western US are largely contributed by high background ozone and frequent downward mixing, while local anthropogenic influences are relatively small (Zhang et al., 2014; Dayan et al., 2017; Jaffe et al., 2018). Frequent downward subsidence of ozone-rich air in the free troposphere that may occur at any time of the day can bring external ozone input to the mountainous surface, resulting in high NOE frequencies there. In other regions over Europe and US, we see much lower NOE event frequencies on average. This is because the daytime peak ozone is relatively lower than those over China, leading to low nighttime ozone concentrations in the residual layer (as indicated by the afternoon ozone at surface of 30 ppbv or less)~~.~~. In addition, nighttime NO emissions there are low, which contributes to weak titration effect (as indicated by the small difference between nighttime ozone and O_x level). As such, the ozone difference between the surface and the residual layer is less stark, and residual layer ozone~~are typically low, which~~ cannot serve as an effective source to enhance ozone at the surface even there is strong mixing or transport.

Our analyses above show that the high ozone levels in the nighttime residual layer that largely remained from daytime ozone provide a critical source of nighttime ozone enhancement at the surface. The trigger of a specific NOE event requires the mixing of ozone-rich air from nighttime residual layer to surface, or horizontal transport of ozone-rich air from adjacent regions. Active nighttime transport and vertical mixing of air ~~is~~ are associated with increasing atmospheric instability, which can be quantitatively indicated by friction velocity (U*), planetary boundary layer height (PBLH), and vertical profiles of temperature (Su et al., 2018; Arrillaga et al., 2019; Wang et al., 2019; Shao et al., 2020). We now evaluate the behavior of atmospheric instability and the strength of vertical mixing ~~during~~ in the NOE events versus NNOE events using these physical parameters obtained from the ERA5 dataset (Section 2.3).

Figure ~~5a~~ 6a and ~~5c~~ 6c compares the evolution of U* and PBLH at the five representative cities averaged over the NOE events to that over the NNOE events. Increasing U* and PBLH levels typically indicate a more unstable boundary layer and thus stronger atmospheric mixing. We ~~do not~~ find that ~~significant differences in~~ the absolute values of nighttime U* and PBLH are generally larger in ~~between~~ the NOE ~~and~~ than NNOE events (Figure S~~4~~5)~~., however~~More importantly, we see distinct differences in their temporal evolution. U* and PBLH typically show a steady decreasing trend throughout the nighttime during NNOE events, while ~~in the NOE events~~ the U* and PBLH show increase in at least a certain part of the nighttime period in the NOE events, suggesting that atmospheric mixing is becoming more active (Figure ~~5a~~ 6a and ~~5c~~6c).

We then calculate the frequency of U* and PBLH increase within two hours before the occurrence time of an NOE event to see whether the increases in ~~FV~~ U* and PBLH are consistently found in most of the NOE events across all sites. Using two hours instead of one is because the response of ozone can be lagged behind the enhanced atmospheric mixing. As shown in Figure ~~5b~~ 6b and Figure ~~5d~~6d, 70% (65%) of the NOE events are associated with an increase in U* (PBLH) averaged at all 814 sites in 2014-2019, supporting that increasing atmospheric instability is critical for the trigger of NOE events. The enhanced atmospheric instability, as indicated by the rise in U* and PBLH values, not only enhance the activity of turbulence and vertical mixing that promotes the downward mixing of ozone-rich air mass from the residual layer to surface, but also dilutes the concentration of NO_x and weaken the titration effect. The combine effects of mixing-induced ozone enhancement and weakened titration-induced ozone loss increase the probability of NOE events. This also explains the sharper decrease in NO_2 and CO during NOE events than the NNOE events as shown in Figure 4, as NO_2 and CO concentrations are much lower in the nighttime residual layer than at the surface. We also find higher frequency of nighttime U* and PBLH enhancement in the warm season than that in the cold season, suggesting that seasonal difference in nighttime atmospheric mixing activity also contributes to that in NOE frequency as shown in Figure 2.

The enhanced atmospheric instability and vertical mixing in the NOE events can be further supported by the differences in the evolution of vertical potential temperature profiles during the NOE events versus NNOE events, as shown in Figure ~~6~~7. Here we use potential temperature as the metric because it describes the efficiency of heat exchange between the land and

near-surface atmosphere. During the NOE events, at all the five representative cities, the decreases in potential temperature with time driven by long-wave radiation cooling extend from the ground to 700 hPa or higher, reflecting effective heat exchange between the land and near-surface atmosphere and thus more active mixing. In comparison, the potential temperature decreases are largely limited in the lowest 100 hPa during the NNOE events, indicating stable and shallow nighttime boundary layer which is not favorable for mixing of air pollutants. The higher potential temperature in Urumqi in NOE than NNOE events is due to the higher NOE frequency in May-August when temperature is significantly higher than April and September.

Previous studies also showed that horizontal transport of ozone-rich air from polluted region can lead to episodic NOE events (Sousa et al., 2011; Ghosh et al., 2013; He et al., 2021). We expect that horizontal transport contributes to ozone enhancement in a specific area if there is higher ozone level upwind. The ozone transport efficiency and magnitude are dependent on the ozone gradient between the source and receptor, and the transport pathway and distance that is closely relevant to the rapid-shift weather conditions. In addition, efficient horizontal transport is typically driven by synoptic processes that may also involve enhanced vertical mixing. These characteristics make it hard to classify the contribution of horizontal transport to NOE events at the national scale, but we will explore their role in the case studies below.

3.3 Case studies of NOE events

The above analyses have illustrated that the high afternoon ozone produced from intensive anthropogenic emissions provide rich ozone in the nighttime residual layer, leading to the overall higher frequency of NOE events in China especially in the industrialized regions compared to other regions, and the enhanced mixing of ozone-rich air in the nighttime residual layer to the surface is a critical mechanism to trigger NOE events. We now present three cases of NOE events at Beijing (representative of the NCP region) and Guangzhou (representative of the PRD region) to zoom in what specific synoptic processes may contribute to the increase in vertical mixing and trigger NOE events.

Figure 8 shows a NOE event observed on July 29, 2015 at multiple sites in Beijing triggered by a convective system. Ozone levels in Beijing exceeded 120 ppbv in the afternoon, decreased rapidly with the sunset, and started increase at around 23:00 LT. The magnitude of this NOE event was up to 36 ppbv with the nighttime peak value exceeding 70 ppbv.

We find that at all sites the nocturnal ozone increases were accompanied with sharp decrease in NO_2 and CO concentrations and an increase in PBLH, a typical signal of enhanced vertical mixing from the ozone-rich air in the residual layer. The large hourly precipitation of 8.4 mm at 23:00 LT indicates that there was a convective storm with the occurrence of NOE event, and we also find a follow-up decrease in the equivalent potential temperature (θ_{se}, derived from temperature and relative humidity), a typical feature of the downdrafts in convective storms (Figure 8d) (Jia et al., 2015; Zhu et al., 2020). Examination of the large-scale synoptic pattern suggests that this convective storm was triggered by a cold vortex. Beijing

11

was located in the periphery of subtropical high at 500 hPa, and was strongly influenced by southwest warm-wet flow which transported abundant water vapor to Beijing (Figure ~~S6~~S5). Analyses of vertical velocity in Figure ~~8~~S6 show that there was strong upward movement before 23:00 LT, lifting warm and moist air and facilitating the formation of convective storms. With the start of rainfall, the precipitation particles fell into the dry air below, and downdrafts were strengthened via evaporative cooling, motivated the transport of ozone from upper layers to surface. The case thus illustrates that strengthened downdrafts and vertical mixing triggered by convective storms is a driver of NOE events. Jia et al. (2015) and Zhu et al. (2020) also presented cases of convective storm-induced NOE events with similar evolution of NO_2, CO, and meteorological parameters in summer in the NCP region.

Figure 9 shows a case of NOE event under the influence of boundary-layer low-level jets in Beijing on August 26, 2017. Nocturnal ozone concentration started increase at 21:00 LT, flatted at 23:00 LT, and increased again at 02:00 LT. The magnitude of the NOE event was 22 ppb hour^{-1}. In this NOE case, the nighttime peak ozone concentrations (about 50 ppbv) were even higher than the afternoon ozone concentrations (30 ppbv), suggesting that there was external ozone source besides the daytime ozone remaining in the nighttime residual layer. We find a subsidence branch of air above the Beijing city in this event, which may bring ozone-rich air from the middle troposphere to lower troposphere (Figure ~~10~~S7).

Both periods with ozone increases in this event were associated with enhanced PBLH and U* values and declined NO_2 and CO levels, again indicating enhanced vertical mixing from air in the upper layer to the surface. Analyses of wind profile show that the wind speed continued increasing and exceeded 10 m s^{-1} in the lower troposphere, shaping a strong vertical wind shear, a typical feature of low-level jets (Figure 9e and Figure ~~S7~~S8). The low-level jets and associated wind shear have been shown to produce turbulent kinetic energy, weaken the decoupling of the residual layer and the stable nighttime boundary layer, and aggravate vertical mixing (Banta et al., 2003; Tsiringakis et al., 2022) . We find that the first period of ozone increase in 21:00-23:00 LT was associated with the strengthening of the low-level jets as indicated by the rapid increase in the wind speed from 10 to 13 m s^{-1}. There were little increases in wind speed from 23:00-01:00, and correspondently no significant ozone increases in this period. The second period of ozone increases was again with the strengthening of low-level jets with wind speed exceeding 20 m s^{-1} from 800 hPa to 975 hPa (Figure 9e). This case thus presents how the development of boundary layer low-level jets triggers NOE events. The low-level jets have also been identified as a key factor causing multiple NOE events in different regions in the NCP region (Zhu et al., 2020), US (Kuang et al., 2011; Hu et al., 2013; Sullivan et al., 2017; Caputi et al., 2019), and Europe (Kulkarni et al., 2016; Klein et al., 2019).

Figure 1~~1~~0 also illustrates a low-level jet~~s~~ induced NOE event in Guangzhou in the southern China on September 21th, 2014. The afternoon ozone concentrations in Guangzhou reached about 60 ppb. The nocturnal ozone exhibited continuously increases from 21:00 LT to 04:00 LT with increases in PBLH and decrease in NO_2 concentration, lifting surface ozone level

from 9 ppbv to 34 ppbv. We find clear development of the low-level jet~~s~~ and wind shear from the wind profiles that can enhance atmospheric mixing as discussed above (Figure 10~~1~~b).

We further notice that the nocturnal ozone enhancement in this case was not only limited in Guangzhou city, but was instead spread at multiple sites in the PRD region at a background of strong northerly winds produced by the typhoon "Fung-wong" (Figure 10~~1~~c). "Fung-wong" is located in the east of the PRD region, and the PRD region is exposed to the northerly wind of its circulation (Figure ~~S8~~S9). Descending air in the periphery of the typhoon can trigger vertical transport of O$_3$-rich air from upper troposphere or even lower stratosphere to the surface, contributing to ozone enhancement (Jiang et al., 2015). More importantly, ~~T~~the nocturnal ozone started increase at sites north to Guangzhou city from 21:00 LT, and gradually propagated to Guangzhou and the southern sites afterward. Figure 1~~d~~e indicates that the mean nighttime ozone concentrations are typically below 25 ppbv in the PRD and its northern surrounding regions. However, we find that in this specific case ozone concentrations at sites north to the PRD region reach 40 ppbv, much higher than those over the PRD region (Figure 10~~1~~d). The northerly winds in the background of typhoon circulation are expected to transport the ozone-rich air in the north to the PRD region, contributing to nocturnal ozone enhancement there. This is also supported by the backward trajectory analyses using the Hybrid Single Particle Lagrangian Integrated Trajectory (HYSPLIT) model (Figure 10~~1~~d). The analysis above thus illustrates that horizontal transport may also contribute to in the NOE event~~s~~, quantifying the relative contribution from vertical mixing versus horizontal transport to ozone enhancement would require modelling studies~~.~~.

3.4 Implications for ozone evolution in the next day

We also examine whether NOE events would have clear instruction to predict daytime ozone of the next day in China. Figure 4 shows that in the five representative cities, the occurrence of NOE events tends to induce higher ozone in the early morning in the next day, compared to the NNOE events. However, it does not necessarily result in higher daytime ozone compared to the precedent day, which highly depends on the timing and strength of the NOE event and the variations of ozone precursors and redistribution in the vertical direction. We find that the frequency of daytime ozone increase or decrease in the day following an NOE event is roughly equivalent (46% vs 54%) for all sites in China. Previous studies have shown that ozone in the nighttime residual layer influenced surface ozone levels in the following day by fumigation of ozone in the residual layer into the developing daytime boundary layer. While the enhanced nocturnal mixing between the residual layer and nighttime boundary layer contribute to nocturnal ozone enhancement at the surface, the enhanced ozone is also subject to more efficient chemical destruction and dry deposition, resulting in lower ozone peak values on the next day (Hu et al., 2013; Caputi et al., 2019). As such, whether NOE events would increase or decrease the ozone level and integrated ozone exposure in the following day is yet to be determined. Analyzing the implication of NOE events in the next day's ozone level will need to further separate the daily variation of ozone from shifts in meteorological conditions and the resulting impacts on ozone chemistry and transport. This would be an important topic of ozone air quality research over China in the future.

13

4 Conclusion

In this study, we report the previously unrecognized high frequency of the NOE events in China, present their statistical characteristics, and explore the possible mechanisms based on six-year (2014-2019) observations from the Chinese national monitoring network. We find that the annual mean frequency of NOE events is 41±10% averaged over all 814 Chinese sites in 2014-2019, which is 46% larger than those over Europe and US. Sites with high frequency (>50%) of NOE events are concentrated in industrialized city clusters (NCP, YRD, and PRD) and in the western China. The NOE frequency is higher in the warm (46%) than the cold season (36%) in most regions, except for the PRD region where NOE events occur at higher frequency in the cold season than in the warm season, consistent with the seasonal evolution of ozone levels. The mean ozone peak during NOE events in the warm season is 37±6 ppbv (31±6 ppbv in the cold season), significantly higher than those in the NNOE events of 17±11 ppbv (10± 9 ppbv), and is sufficiently high to pose negative impacts on human health and vegetation activity. In about 85% of the NOE events the maximum ozone enhancement during NOE events is within 5-15 ppbv hour^{-1}, but in 10% of the cases the ozone increase can exceed 20 ppbv hour^{-1}. We also find much faster decreasing rate of nighttime NO_2 and CO concentrations and increases in U* and PBLH that are indicative of enhanced atmospheric vertical mixing during NOE events compared to NNOE events.

We propose that the high afternoon ozone provides rich ozone source in the nighttime residual layer, determining the overall higher frequency of NOE events at regions with severe ozone pollution than cleaner regions, and then the enhanced atmospheric mixing trigger NOE events by allowing the ozone-rich air in the residual layer to mix into the nighttime boundary layer. Figure 121 illustrates the conceptual model of the formation of the high NOE frequency over China. High ozone is generated by active photochemistry in the daytime, and has relatively small vertical gradient in the daytime boundary layer with effective vertical mixing and turbulence. At night, the surface ozone decreases significantly due to titration in high NO_x environment and dry deposition with the shallowing of nighttime boundary layer, while relatively higher ozone remains in the residual layer. Synoptic processes such as convective storms and low-level jets produce turbulent kinetic energy, weaken the decoupling of the residual layer and the nighttime boundary layer, and aggravate vertical mixing of ozone-rich air in the residual layer into the nighttime boundary layer and cause the NOE event. This is supported by our analyses that more than 70% (65%) of the NOE events are associated with increases in U* and PBLH values, and also supported by the observed sharper decreases in NO_2 and CO concentrations in NOE events compared to the NNOE events. In addition, horizontal transport of ozone-rich plumes may also be a supplementary driver of NOE event in areas such as the PRD regions.

Our study thus provides a first overview of the NOE events over China from characteristics to mechanisms. Nevertheless, as we focus more on the general behaviors in NOE events based on six-year observations at hundreds of sites than episodic cases, the proposed conceptual diagram of the NOE event mechanism may not cover all the NOE events. We call for more

14

direct observations of vertical structure of ozone and its evolution from daytime to nighttime (Kuang et al., 2011; Jia et al., 2015; Caputi et al., 2019; He et al., 2021), and more 3-D chemical modelling studies (Hu et al., 2013; Klein et al., 2014) to ~~better~~ quantitatively explore the contribution of mixing and regional transport to NOE events (including the underlying synoptic processes such as low-level jets and convective storms), and to further analyze the impacts of NOE events on atmospheric chemistry, human health, and vegetation productivity.

References

Arrillaga, J. A., Yagüe, C., Román-Cascón, C., Sastre, M., Jiménez, M. A., Maqueda, G., and Vilà-Guerau de Arellano, J.: From weak to intense downslope winds: origin, interaction with boundary-layer turbulence and impact on CO_2 variability, Atmos. Chem. Phys., 19, 4615-4635, 10.5194/acp-19-4615-2019, 2019.

Banta, R. M., Pichugina, Y. L., and Newsom, R. K.: Relationship between Low-Level Jet Properties and Turbulence Kinetic Energy in the Nocturnal Stable Boundary Layer, Journal of the Atmospheric Sciences, 60, 2549-2555, 10.1175/1520-0469(2003)060<2549:Rbljpa>2.0.Co;2, 2003.

15

Brown, S. S. and Stutz, J.: Nighttime radical observations and chemistry, Chemical Society Reviews, 41, 6405-6447, 10.1039/C2CS35181A, 2012.

495   Caputi, D. J., Faloona, I., Trousdell, J., Smoot, J., Falk, N., and Conley, S.: Residual layer ozone, mixing, and the nocturnal jet in California's San Joaquin Valley, Atmos. Chem. Phys., 19, 4721-4740, 10.5194/acp-19-4721-2019, 2019.

Cooper, O. R., Gao, R.-S., Tarasick, D., Leblanc, T., and Sweeney, C.: Long-term ozone trends at rural ozone monitoring sites across the United States, 1990–2010, Journal of Geophysical Research: Atmospheres, 117, https://doi.org/10.1029/2012JD018261, 2012.

500   Cordeiro, G. D., Liporoni, R., Caetano, C. A., Krug, C., Martínez-Martínez, C. A., Martins, H. O. J., Cardoso, R. K. O. A., Araujo, F. F., Araújo, P. C. S., Oliveira, R., Schlindwein, C., Warrant, E. J., Dötterl, S., and Alves-dos-Santos, I.: Nocturnal Bees as Crop Pollinators, Agronomy, 11, 1014, 2021.

Dayan, U., Ricaud, P., Zbinden, R., and Dulac, F.: Atmospheric pollution over the eastern Mediterranean during summer – a review, Atmos. Chem. Phys., 17, 13233-13263, 10.5194/acp-17-13233-2017, 2017.

505   De Moraes, C. M., Mescher, M. C., and Tumlinson, J. H.: Caterpillar-induced nocturnal plant volatiles repel conspecific females, Nature, 410, 577-580, 10.1038/35069058, 2001.

Eliasson, I., Thorsson, S., and Andersson-Sköld, Y.: Summer nocturnal ozone maxima in Göteborg, Sweden, Atmospheric Environment, 37, 2615-2627, https://doi.org/10.1016/S1352-2310(03)00205-X, 2003.

Feng, Z., Xu, Y., Kobayashi, K., Dai, L., Zhang, T., Agathokleous, E., Calatayud, V., Paoletti, E., Mukherjee, A., Agrawal, 510   M., Park, R. J., Oak, Y. J., and Yue, X.: Ozone pollution threatens the production of major staple crops in East Asia, Nature Food, 3, 47-56, 10.1038/s43016-021-00422-6, 2022.

Fleming, Z. L., Doherty, R. M., von Schneidemesser, E., Malley, C. S., Cooper, O. R., Pinto, J. P., Colette, A., Xu, X., Simpson, D., Schultz, M. G., Lefohn, A. S., Hamad, S., Moolla, R., Solberg, S., and Feng, Z.: Tropospheric Ozone Assessment Report: Present-day ozone distribution and trends relevant to human health, Elementa: Science of the 515   Anthropocene, 6, 10.1525/elementa.273, 2018.

Gao, M., Gao, J., Zhu, B., Kumar, R., Lu, X., Song, S., Zhang, Y., Jia, B., Wang, P., Beig, G., Hu, J., Ying, Q., Zhang, H., Sherman, P., and McElroy, M. B.: Ozone pollution over China and India: seasonality and sources, Atmos. Chem. Phys., 20, 4399-4414, 10.5194/acp-20-4399-2020, 2020.

Ghosh, D., Lal, S., and Sarkar, U.: High nocturnal ozone levels at a surface site in Kolkata, India: Trade-off between 520   meteorology and specific nocturnal chemistry, Urban Climate, 5, 82-103, https://doi.org/10.1016/j.uclim.2013.07.002, 2013.

Guo, H., Gu, X., Ma, G., Shi, S., Wang, W., Zuo, X., and Zhang, X.: Spatial and temporal variations of air quality and six air pollutants in China during 2015-2017, Sci Rep, 9, 15201, 10.1038/s41598-019-50655-6, 2019.

He, Y., Wang, H., Wang, H., Xu, X., Li, Y., and Fan, S.: Meteorology and topographic influences on nocturnal ozone 525   increase during the summertime over Shaoguan, China, Atmospheric Environment, 256, 118459, https://doi.org/10.1016/j.atmosenv.2021.118459, 2021.

Hersbach, H., Bell, B., Berrisford, P., Hirahara, S., Horányi, A., Muñoz-Sabater, J., Nicolas, J., Peubey, C., Radu, R., Schepers, D., Simmons, A., Soci, C., Abdalla, S., Abellan, X., Balsamo, G., Bechtold, P., Biavati, G., Bidlot, J., Bonavita, M., De Chiara, G., Dahlgren, P., Dee, D., Diamantakis, M., Dragani, R., Flemming, J., Forbes, R.,

530   Fuentes, M., Geer, A., Haimberger, L., Healy, S., Hogan, R. J., Hólm, E., Janisková, M., Keeley, S., Laloyaux, P., Lopez, P., Lupu, C., Radnoti, G., de Rosnay, P., Rozum, I., Vamborg, F., Villaume, S., and Thépaut, J.-N.: The ERA5 global reanalysis, Quarterly Journal of the Royal Meteorological Society, 146, 1999-2049, https://doi.org/10.1002/qj.3803, 2020.

Hu, X.-M., Doughty, D. C., Sanchez, K. J., Joseph, E., and Fuentes, J. D.: Ozone variability in the atmospheric boundary

535   layer in Maryland and its implications for vertical transport model, Atmospheric Environment, 46, 354-364, https://doi.org/10.1016/j.atmosenv.2011.09.054, 2012.

Hu, X.-M., Klein, P. M., Xue, M., Zhang, F., Doughty, D. C., Forkel, R., Joseph, E., and Fuentes, J. D.: Impact of the vertical mixing induced by low-level jets on boundary layer ozone concentration, Atmospheric Environment, 70, 123-130, https://doi.org/10.1016/j.atmosenv.2012.12.046, 2013.

540 Huang, X., Ding, A., Gao, J., Zheng, B., Zhou, D., Qi, X., Tang, R., Wang, J., Ren, C., Nie, W., Chi, X., Xu, Z., Chen, L., Li, Y., Che, F., Pang, N., Wang, H., Tong, D., Qin, W., Cheng, W., Liu, W., Fu, Q., Liu, B., Chai, F., Davis, S. J., Zhang, Q., and He, K.: Enhanced secondary pollution offset reduction of primary emissions during COVID-19 lockdown in China, National Science Review, 8, 10.1093/nsr/nwaa137, 2020.

Jacob, D. J.: Heterogeneous chemistry and tropospheric ozone, Atmospheric Environment, 34, 2131-2159,

545   https://doi.org/10.1016/S1352-2310(99)00462-8, 2000.

Jaffe, D. A., Cooper, O. R., Fiore, A. M., Henderson, B. H., Tonnesen, G. S., Russell, A. G., Henze, D. K., Langford, A. O., Lin, M., and Moore, T.: Scientific assessment of background ozone over the U.S.: Implications for air quality management, Elementa: Science of the Anthropocene, 6, 10.1525/elementa.309, 2018.

Jia, S., Xu, X., Lin, W., Wang, Y., He, X., and Hualong, Z.: Increased Mixing Ratio of Surface Ozone by Nighttime

550   Convection Process over the North China Plain, J Appl Meteor Sci, - 26, - 280, - 10.11898/1001-7313.20150303, 2015.

Jiang, Y. C., Zhao, T. L., Liu, J., Xu, X. D., Tan, C. H., Cheng, X. H., Bi, X. Y., Gan, J. B., You, J. F., and Zhao, S. Z.: Why does surface ozone peak before a typhoon landing in southeast China?, Atmos. Chem. Phys., 15, 13331-13338, 10.5194/acp-15-13331-2015, 2015.

555 Jiang, Z., Li, J., Lu, X., Gong, C., Zhang, L., and Liao, H.: Impact of western Pacific subtropical high on ozone pollution over eastern China, Atmos. Chem. Phys., 21, 2601-2613, 10.5194/acp-21-2601-2021, 2021.

Klein, A., Ravetta, F., Thomas, J. L., Ancellet, G., Augustin, P., Wilson, R., Dieudonné, E., Fourmentin, M., Delbarre, H., and Pelon, J.: Influence of vertical mixing and nighttime transport on surface ozone variability in the morning in Paris and the surrounding region, Atmospheric Environment, 197, 92-102,

560   https://doi.org/10.1016/j.atmosenv.2018.10.009, 2019.

17

Klein, P. M., Hu, X.-M., and Xue, M.: Impacts of Mixing Processes in Nocturnal Atmospheric Boundary Layer on Urban Ozone Concentrations, Boundary-Layer Meteorology, 150, 107-130, 10.1007/s10546-013-9864-4, 2014.

Kleinman, L., Daum, P., Lee, Y.-N., Nunnermacker, L., Springston, S., Weinstein-Lloyd, J., and Rudolph, J.: Ozone production efficiency in an urban area, Journal of Geophysical Research, 107, 10.1029/2002JD002529, 2002.

565   Kuang, S., Newchurch, M. J., Burris, J., Wang, L., Buckley, P. I., Johnson, S., Knupp, K., Huang, G., Phillips, D., and Cantrell, W.: Nocturnal ozone enhancement in the lower troposphere observed by lidar, Atmospheric Environment, 45, 6078-6084, https://doi.org/10.1016/j.atmosenv.2011.07.038, 2011.

Kulkarni, P. S., Dasari, H. P., Sharma, A., Bortoli, D., Salgado, R., and Silva, A. M.: Nocturnal surface ozone enhancement over Portugal during winter: Influence of different atmospheric conditions, Atmospheric Environment, 147, 109-

570   120, 10.1016/j.atmosenv.2016.09.056, 2016.

Lefohn, A. S., Malley, C. S., Smith, L., Wells, B., Hazucha, M., Simon, H., Naik, V., Mills, G., Schultz, M. G., Paoletti, E., De Marco, A., Xu, X., Zhang, L., Wang, T., Neufeld, H. S., Musselman, R. C., Tarasick, D., Brauer, M., Feng, Z., Tang, H., Kobayashi, K., Sicard, P., Solberg, S., and Gerosa, G.: Tropospheric ozone assessment report: Global ozone metrics for climate change, human health, and crop/ecosystem research, Elementa: Science of the

575   Anthropocene, 6, 10.1525/elementa.279, 2018.

Li, D., Shindell, D., Ding, D., Lu, X., Zhang, L., and Zhang, Y.: Surface ozone impacts on major crop production in China from 2010 to 2017, Atmos. Chem. Phys., 22, 2625-2638, 10.5194/acp-22-2625-2022, 2022.

Li, K., Jacob, D. J., Liao, H., Qiu, Y., Shen, L., Zhai, S., Bates, K. H., Sulprizio, M. P., Song, S., Lu, X., Zhang, Q., Zheng, B., Zhang, Y., Zhang, J., Lee, H. C., and Kuk, S. K.: Ozone pollution in the North China Plain spreading into the

580   late-winter haze season, Proceedings of the National Academy of Sciences, 118, e2015797118, doi:10.1073/pnas.2015797118, 2021.

Lin, J., Youn, D., Liang, X., and Wuebbles, D.: Global model simulation of summertime U.S. ozone diurnal cycle and its sensitivity to PBL mixing, spatial resolution, and emissions, Atmospheric Environment, 42, 8470-8483, 10.1016/j.atmosenv.2008.08.012, 2008.

585   Liu, Y. and Wang, T.: Worsening urban ozone pollution in China from 2013 to 2017 – Part 1: The complex and varying roles of meteorology, Atmos. Chem. Phys., 20, 6305-6321, 10.5194/acp-20-6305-2020, 2020.

Lu, X., Zhang, L., Wang, X., Gao, M., Li, K., Zhang, Y., Yue, X., and Zhang, Y.: Rapid Increases in Warm-Season Surface Ozone and Resulting Health Impact in China Since 2013, Environmental Science & Technology Letters, 7, 240-247, 10.1021/acs.estlett.0c00171, 2020.

590   Lu, X., Hong, J., Zhang, L., Cooper, O. R., Schultz, M. G., Xu, X., Wang, T., Gao, M., Zhao, Y., and Zhang, Y.: Severe Surface Ozone Pollution in China: A Global Perspective, Environmental Science & Technology Letters, 5, 487-494, 10.1021/acs.estlett.8b00366, 2018.

Lu, X., Ye, X., Zhou, M., Zhao, Y., Weng, H., Kong, H., Li, K., Gao, M., Zheng, B., Lin, J., Zhou, F., Zhang, Q., Wu, D., Zhang, L., and Zhang, Y.: The underappreciated role of agricultural soil nitrogen oxide emissions in ozone pollution regulation in North China, Nature Communications, 12, 5021, 10.1038/s41467-021-25147-9, 2021.

Millet, D. B., Baasandorj, M., Hu, L., Mitroo, D., Turner, J., and Williams, B. J.: Nighttime Chemistry and Morning Isoprene Can Drive Urban Ozone Downwind of a Major Deciduous Forest, Environ Sci Technol, 50, 4335-4342, 10.1021/acs.est.5b06367, 2016.

Monks, P. S., Archibald, A. T., Colette, A., Cooper, O., Coyle, M., Derwent, R., Fowler, D., Granier, C., Law, K. S., Mills, G. E., Stevenson, D. S., Tarasova, O., Thouret, V., von Schneidemesser, E., Sommariva, R., Wild, O., and Williams, M. L.: Tropospheric ozone and its precursors from the urban to the global scale from air quality to short-lived climate forcer, Atmos. Chem. Phys., 15, 8889-8973, 10.5194/acp-15-8889-2015, 2015.

Reitebuch, O., Strassburger, A., Emeis, S., and Kuttler, W.: Nocturnal secondary ozone concentration maxima analysed by sodar observations and surface measurements, Atmospheric Environment, 34, 4315-4329, https://doi.org/10.1016/S1352-2310(00)00185-0, 2000.

Shao, Y., Zhang, J., Ishizuka, M., Mikami, M., Leys, J., and Huang, N.: Dependency of particle size distribution at dust emission on friction velocity and atmospheric boundary-layer stability, Atmos. Chem. Phys., 20, 12939-12953, 10.5194/acp-20-12939-2020, 2020.

Sillman, S.: The use of NO y , H2O2, and HNO3 as indicators for ozone-NO x -hydrocarbon sensitivity in urban locations, Journal of Geophysical Research: Atmospheres, 100, 14175-14188, https://doi.org/10.1029/94JD02953, 1995.

Škerlak, B., Sprenger, M., and Wernli, H.: A global climatology of stratosphere–troposphere exchange using the ERA-Interim data set from 1979 to 2011, Atmos. Chem. Phys., 14, 913-937, 10.5194/acp-14-913-2014, 2014.

Sousa, S. I. V., Alvim-Ferraz, M. C. M., and Martins, F. G.: Identification and origin of nocturnal ozone maxima at urban and rural areas of Northern Portugal – Influence of horizontal transport, Atmospheric Environment, 45, 942-956, https://doi.org/10.1016/j.atmosenv.2010.11.008, 2011.

Stohl, A., Bonasoni, P., Cristofanelli, P., Collins, W., Feichter, J., Frank, A., Forster, C., Gerasopoulos, E., Gäggeler, H., James, P., Kentarchos, T., Kromp-Kolb, H., Krüger, B., Land, C., Meloen, J., Papayannis, A., Priller, A., Seibert, P., Sprenger, M., Roelofs, G. J., Scheel, H. E., Schnabel, C., Siegmund, P., Tobler, L., Trickl, T., Wernli, H., Wirth, V., Zanis, P., and Zerefos, C.: Stratosphere-troposphere exchange: A review, and what we have learned from STACCATO, Journal of Geophysical Research: Atmospheres, 108, https://doi.org/10.1029/2002JD002490, 2003.

Strode, S. A., Ziemke, J. R., Oman, L. D., Lamsal, L. N., Olsen, M. A., and Liu, J.: Global changes in the diurnal cycle of surface ozone, Atmospheric Environment, 199, 323-333, 10.1016/j.atmosenv.2018.11.028, 2019.

Su, T., Li, Z., and Kahn, R.: Relationships between the planetary boundary layer height and surface pollutants derived from lidar observations over China: regional pattern and influencing factors, Atmos. Chem. Phys., 18, 15921-15935, 10.5194/acp-18-15921-2018, 2018.
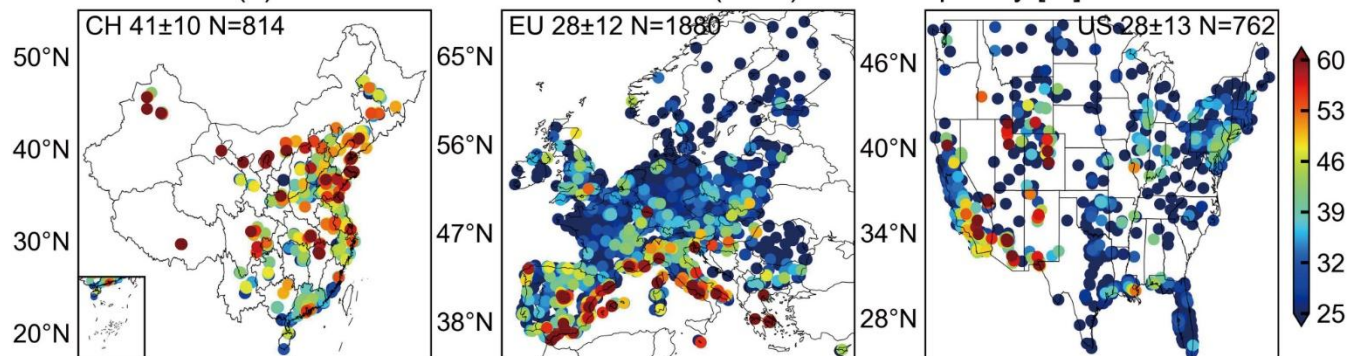
Sullivan, J. T., Rabenhorst, S. D., Dreessen, J., McGee, T. J., Delgado, R., Twigg, L., and Sumnicht, G.: Lidar observations revealing transport of O3 in the presence of a nocturnal low-level jet: Regional implications for "next-day" pollution, Atmospheric Environment, 158, 160-171, https://doi.org/10.1016/j.atmosenv.2017.03.039, 2017.

Tan, Z., Ma, X., Lu, K., Jiang, M., Zou, Q., Wang, H., Zeng, L., and Zhang, Y.: Direct evidence of local photochemical production driven ozone episode in Beijing: A case study, Science of The Total Environment, 800, 148868, https://doi.org/10.1016/j.scitotenv.2021.148868, 2021.

Tsiringakis, A., Theeuwes, N. E., Barlow, J. F., and Steeneveld, G.-J.: Interactions Between the Nocturnal Low-Level Jets and the Urban Boundary Layer: A Case Study over London, Boundary-Layer Meteorology, 10.1007/s10546-021-00681-7, 2022.

Turner, M. C., Jerrett, M., Pope, C. A., 3rd, Krewski, D., Gapstur, S. M., Diver, W. R., Beckerman, B. S., Marshall, J. D., Su, J., Crouse, D. L., and Burnett, R. T.: Long-Term Ozone Exposure and Mortality in a Large Prospective Study, Am J Respir Crit Care Med, 193, 1134-1142, 10.1164/rccm.201508-1633OC, 2016.

Wang, H., Wang, W., Huang, X., and Ding, A.: Impacts of stratosphere-to-troposphere-transport on summertime surface ozone over eastern China, Science Bulletin, 65, 276-279, 10.1016/j.scib.2019.11.017, 2020.

Wang, H., Lu, K., Chen, S., Li, X., Zeng, L., Hu, M., and Zhang, Y.: Characterizing nitrate radical budget trends in Beijing during 2013–2019, Science of The Total Environment, 795, 148869, https://doi.org/10.1016/j.scitotenv.2021.148869, 2021.

Wang, H., Lu, K., Chen, X., Zhu, Q., Wu, Z., Wu, Y., and Sun, K.: Fast particulate nitrate formation via N2O5 uptake aloft in winter in Beijing, Atmos. Chem. Phys., 18, 10483-10495, 10.5194/acp-18-10483-2018, 2018.

Wang, L., Liu, J., Gao, Z., Li, Y., Huang, M., Fan, S., Zhang, X., Yang, Y., Miao, S., Zou, H., Sun, Y., Chen, Y., and Yang, T.: Vertical observations of the atmospheric boundary layer structure over Beijing urban area during air pollution episodes, Atmos. Chem. Phys., 19, 6949-6967, 10.5194/acp-19-6949-2019, 2019.

Wang, T., Xue, L., Brimblecombe, P., Lam, Y. F., Li, L., and Zhang, L.: Ozone pollution in China: A review of concentrations, meteorological influences, chemical precursors, and effects, Science of The Total Environment, 575, 1582-1596, https://doi.org/10.1016/j.scitotenv.2016.10.081, 2017a.

Wang, W.-N., Cheng, T.-H., Gu, X.-F., Chen, H., Guo, H., Wang, Y., Bao, F.-W., Shi, S.-Y., Xu, B.-R., Zuo, X., Meng, C., and Zhang, X.-C.: Assessing Spatial and Temporal Patterns of Observed Ground-level Ozone in China, Scientific Reports, 7, 3651, 10.1038/s41598-017-03929-w, 2017b.

Yue, X., Unger, N., Harper, K., Xia, X., Liao, H., Zhu, T., Xiao, J., Feng, Z., and Li, J.: Ozone and haze pollution weakens net primary productivity in China, Atmos. Chem. Phys., 17, 6073-6089, 10.5194/acp-17-6073-2017, 2017.

Zhang, L., Jacob, D. J., Yue, X., Downey, N. V., Wood, D. A., and Blewitt, D.: Sources contributing to background surface ozone in the US Intermountain West, Atmos. Chem. Phys., 14, 5295-5309, 10.5194/acp-14-5295-2014, 2014.

Zhao, D., Liu, G., Xin, J., Quan, J., Wang, Y., Wang, X., Dai, L., Gao, W., Tang, G., Hu, B., Ma, Y., Wu, X., Wang, L., Liu, Z., and Wu, F.: Haze pollution under a high atmospheric oxidization capacity in summer in Beijing: insights into

660   formation mechanism of atmospheric physicochemical processes, Atmos. Chem. Phys., 20, 4575-4592, 10.5194/acp-20-4575-2020, 2020.
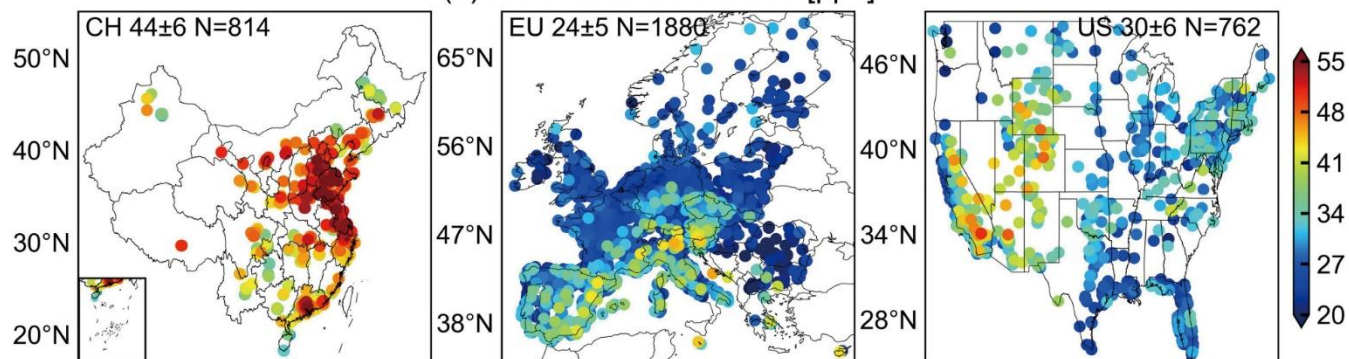
Zhu, X., Ma, Z., Li, Z., Wu, J., Guo, H., Yin, X., Ma, X., and Qiao, L.: Impacts of meteorological conditions on nocturnal surface ozone enhancement during the summertime in Beijing, Atmospheric Environment, 225, 117368, https://doi.org/10.1016/j.atmosenv.2020.117368, 2020.
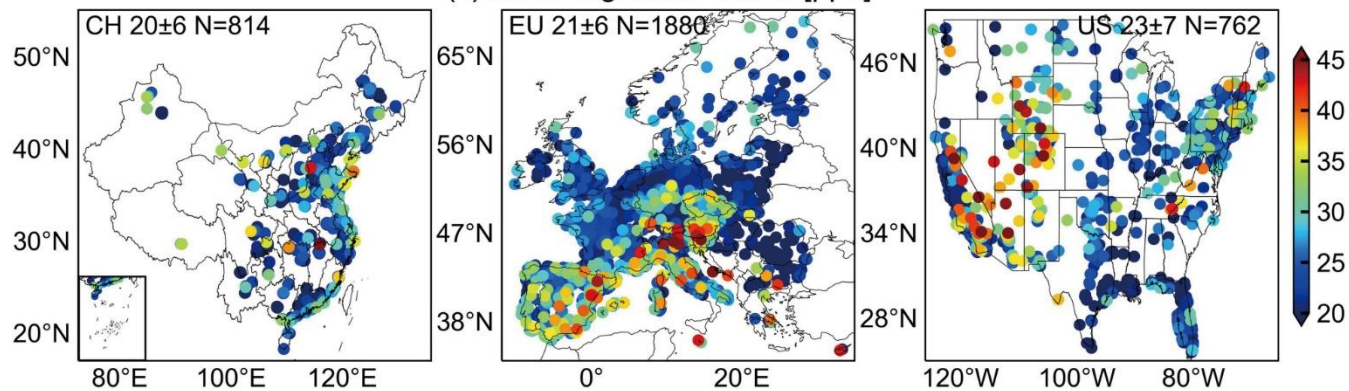
665

(a) Nocturnal ozone enhancement (NOE) event frequency [%]

CH 41±10 N=814   EU 28±12 N=1880   US 28±13 N=762

(b) Mean afternoon ozone [ppb]

CH 44±6 N=814   EU 24±5 N=1880   US 30±6 N=762

(c) Mean nighttime ozone [ppb]

CH 20±6 N=814   EU 21±6 N=1880   US 23±7 N=762

(a) Nocturnal ozone enhancement (NOE) event frequency

CH 41±10 %, N=814   EU 28±12 %, N=1880   US 28±13 %, N=762

(b) Mean afternoon ozone

CH 44±6 ppb, N=814   EU 24±5 ppb, N=1880   US 30±6 ppb, N=762

(c) Mean nighttime O_x

CH 40±6 ppb, N=814   EU 29±5 ppb, N=1880   US 30±5 ppb, N=322

(d) Mean nighttime ozone

CH 20±6 ppb, N=814   EU 21±6 ppb, N=1880   US 23±7 ppb, N=762
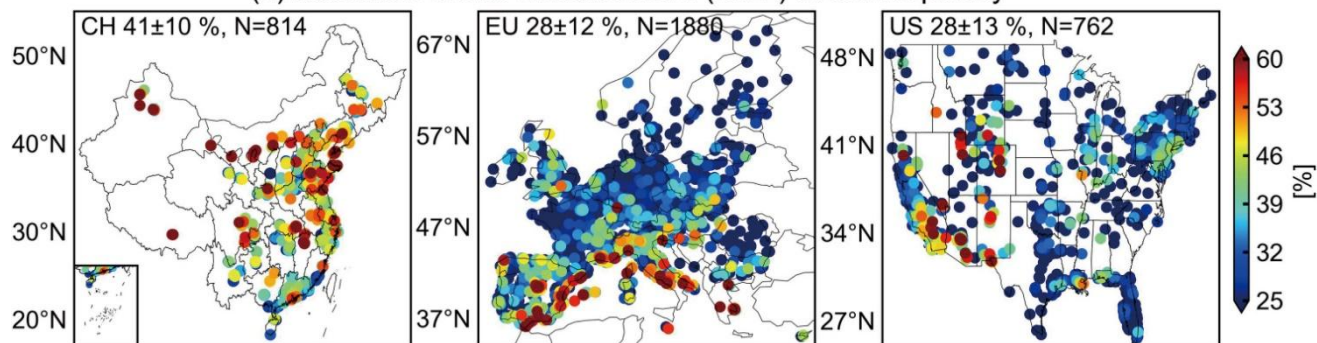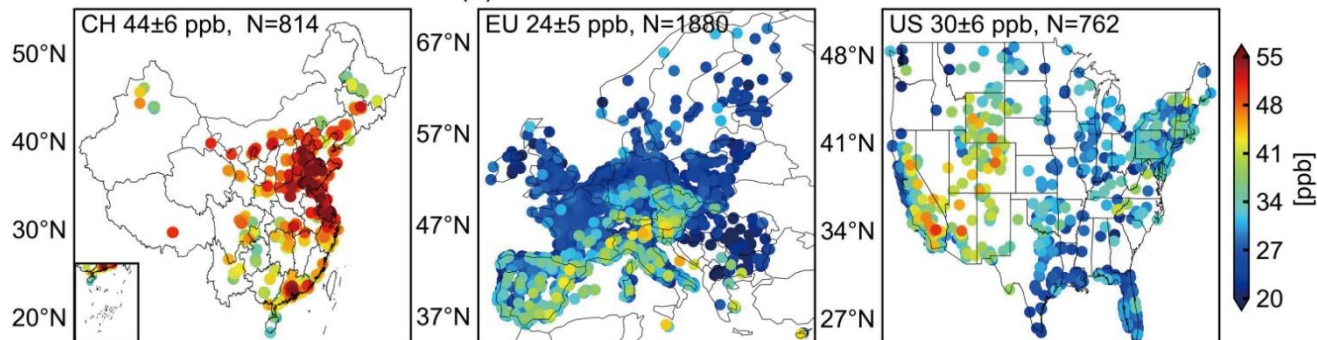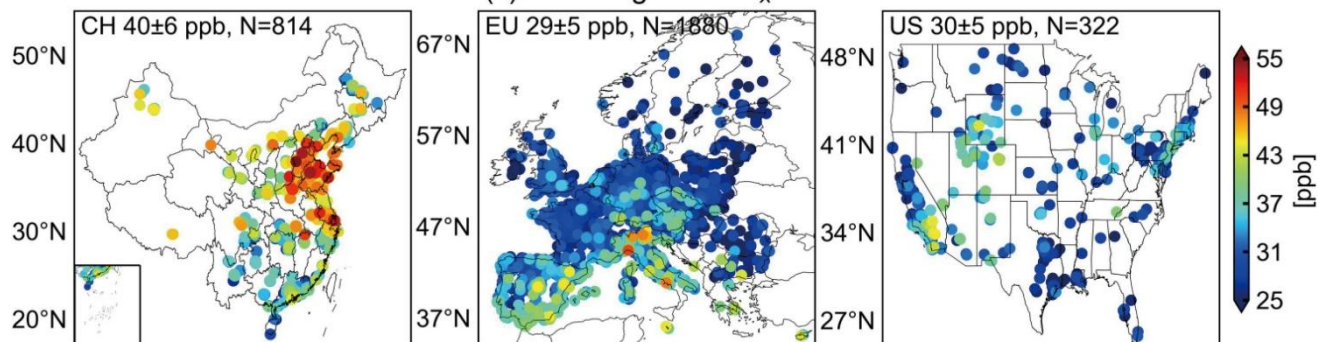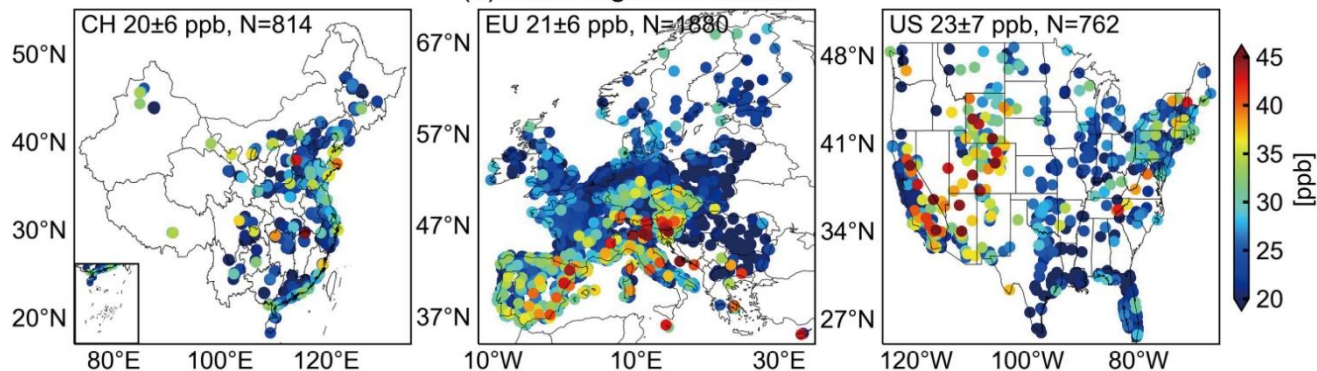
670 **Figure 1.** Comparison of annual frequency of nocturnal ozone enhancement (NOE) event, mean afternoon (14:00-17:00 LT) ozone, and mean nighttime (20:00-06:00 LT) ozone between China (CH), Europe (EU), and the United States (US), averaged over 2014-2019. Only sites with continuous measurements are included. ~~The values of regional mean and standard deviations among the N sites are shown inset at the top of each figure (mean ± standard deviation).~~The regional mean and standard deviations among the N sites are shown inset.

675

24
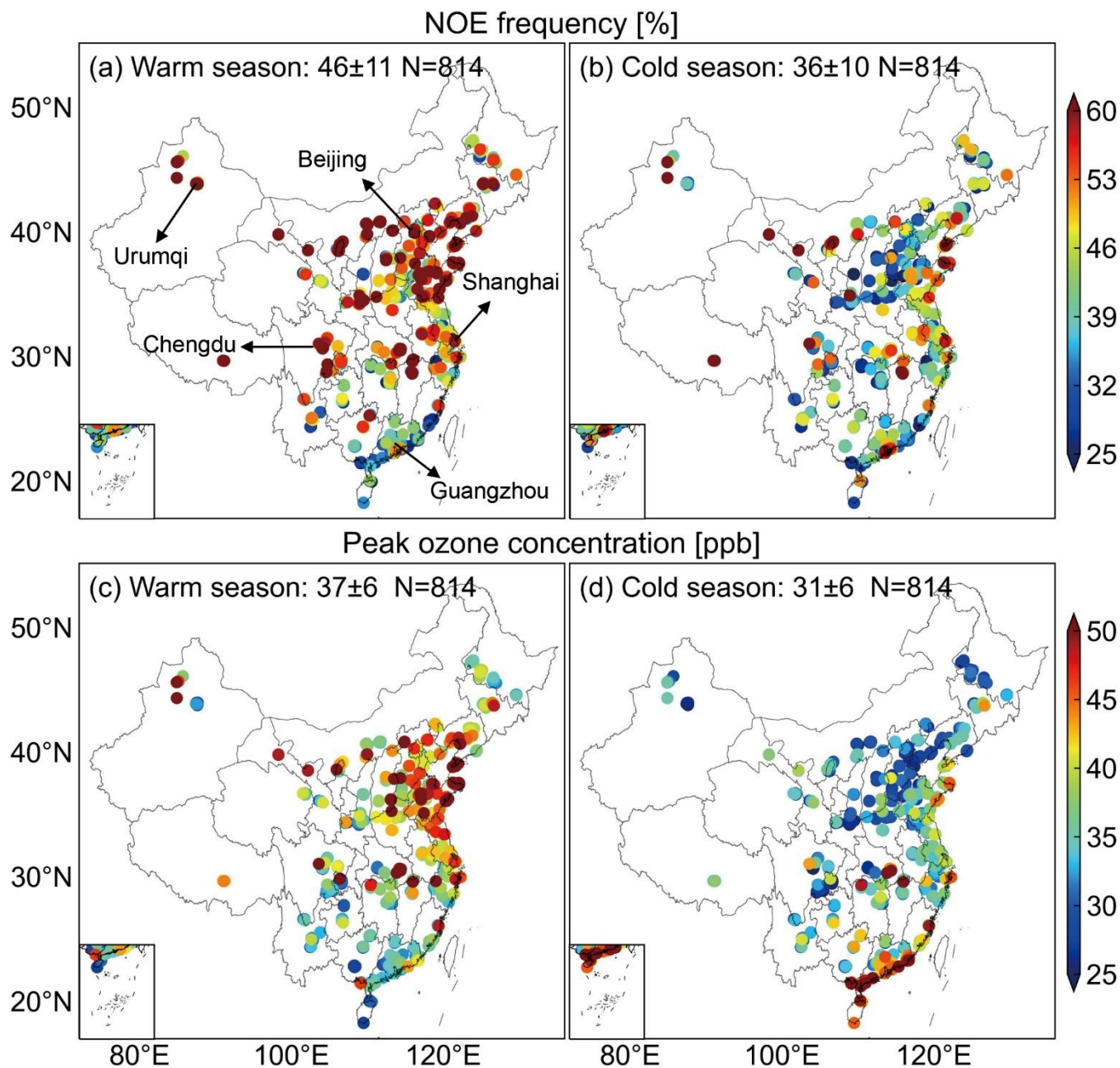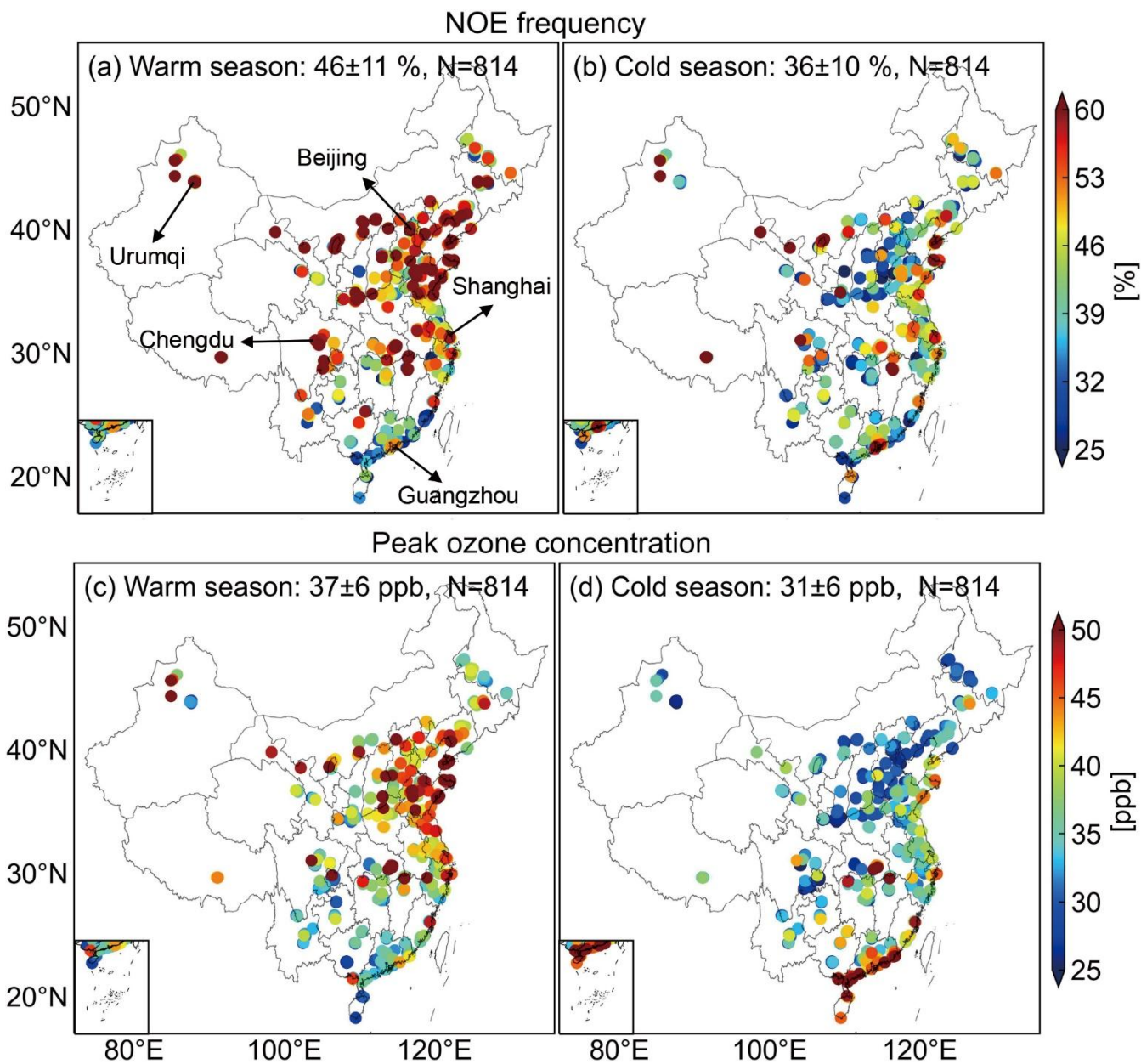
Figure 2. Comparison of the NOE event frequency and nocturnal peak ozone concentrations between the warm season (April-September, panels a and c) and cold season (October-March, panels b and d) in China. The values of regional mean and standard deviations among the N sites are shown inset at the top of each figure (mean ± standard deviation).~~The regional mean and standard deviations among the N sites are shown inset.~~
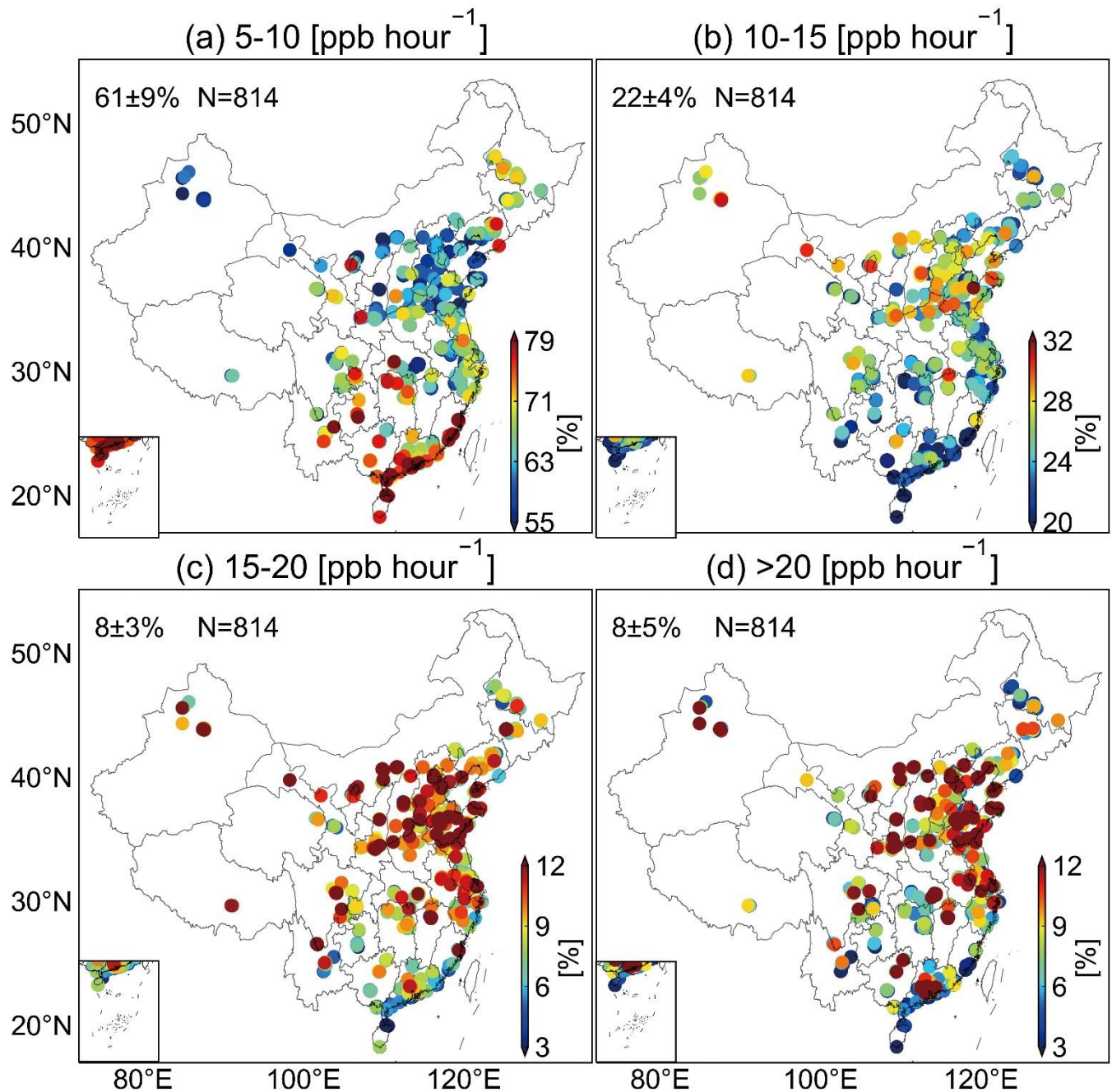
Figure 3. Frequency of different magnitudes of the NOE events (the maximum of $\Delta O_3 / \Delta t$ in an NOE event) in the warm season in China. The values of regional mean and standard deviations among the N sites are shown inset at the top of each figure (mean ± standard deviation).~~The regional mean and standard deviations among the N sites are shown inset.~~

690

NOE occurrence time

NOE events

NNOE events

(a)

18%
29%
23%
19% 11%

Beijing (23%)
O₃ NO₂ CO [ppb]

Beijing (29%)

(b)

35%
21%
13%
13% 18%

Shanghai (27%)

Shanghai (19%)

(c)

28%
26%
22%
14% 10%

Guangzhou (19%)

Guangzhou (22%)

(d)

30%
25%
19%
20% 6%

Chengdu (38%)

Chengdu (13%)

(e)

39%
28%
24%
9%

Urumqi (37%)

Urumqi (6%)

18   22   02   06

Hour (Local time)

22-23   02-03

20-21   00-01   04-05

27
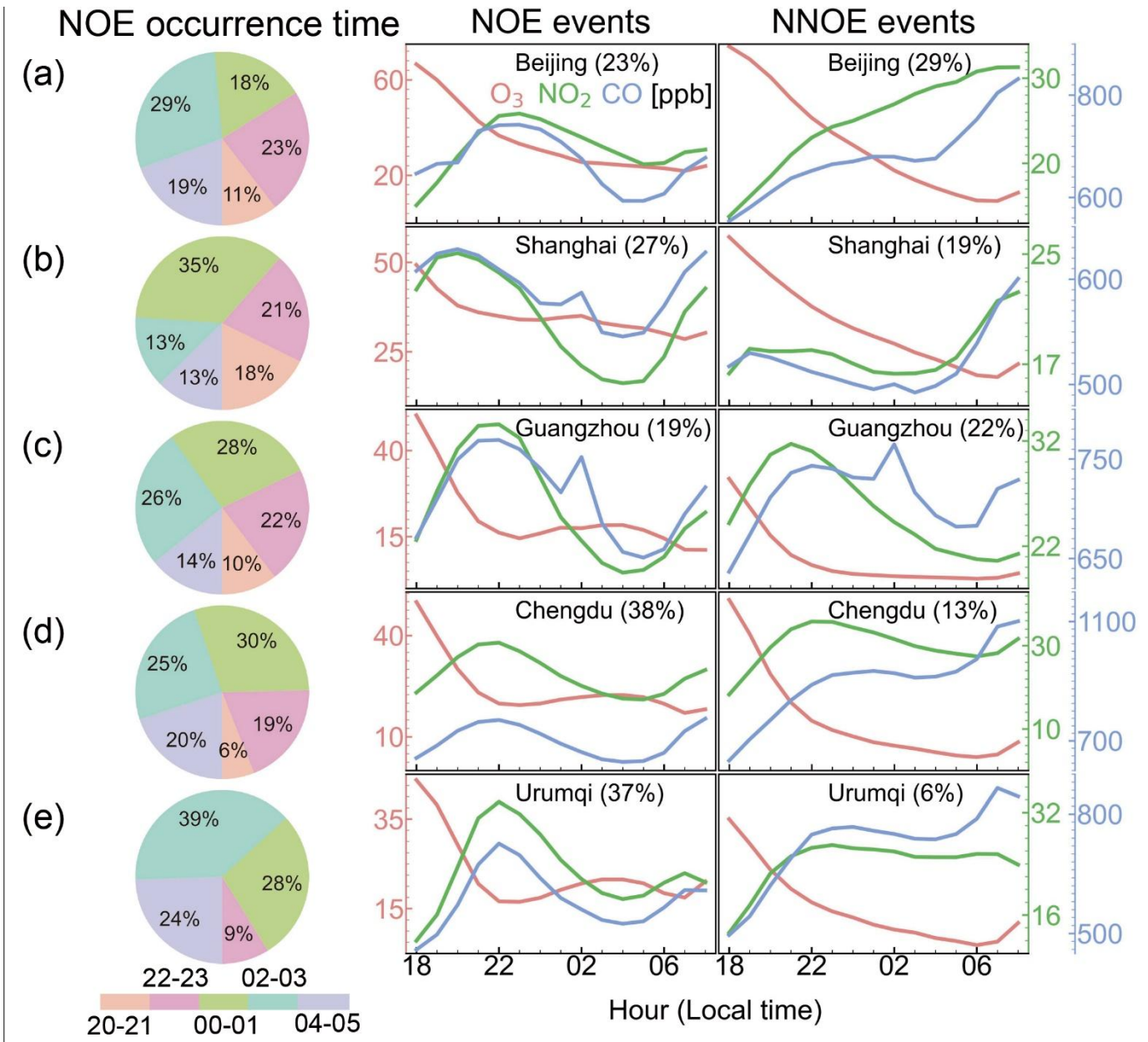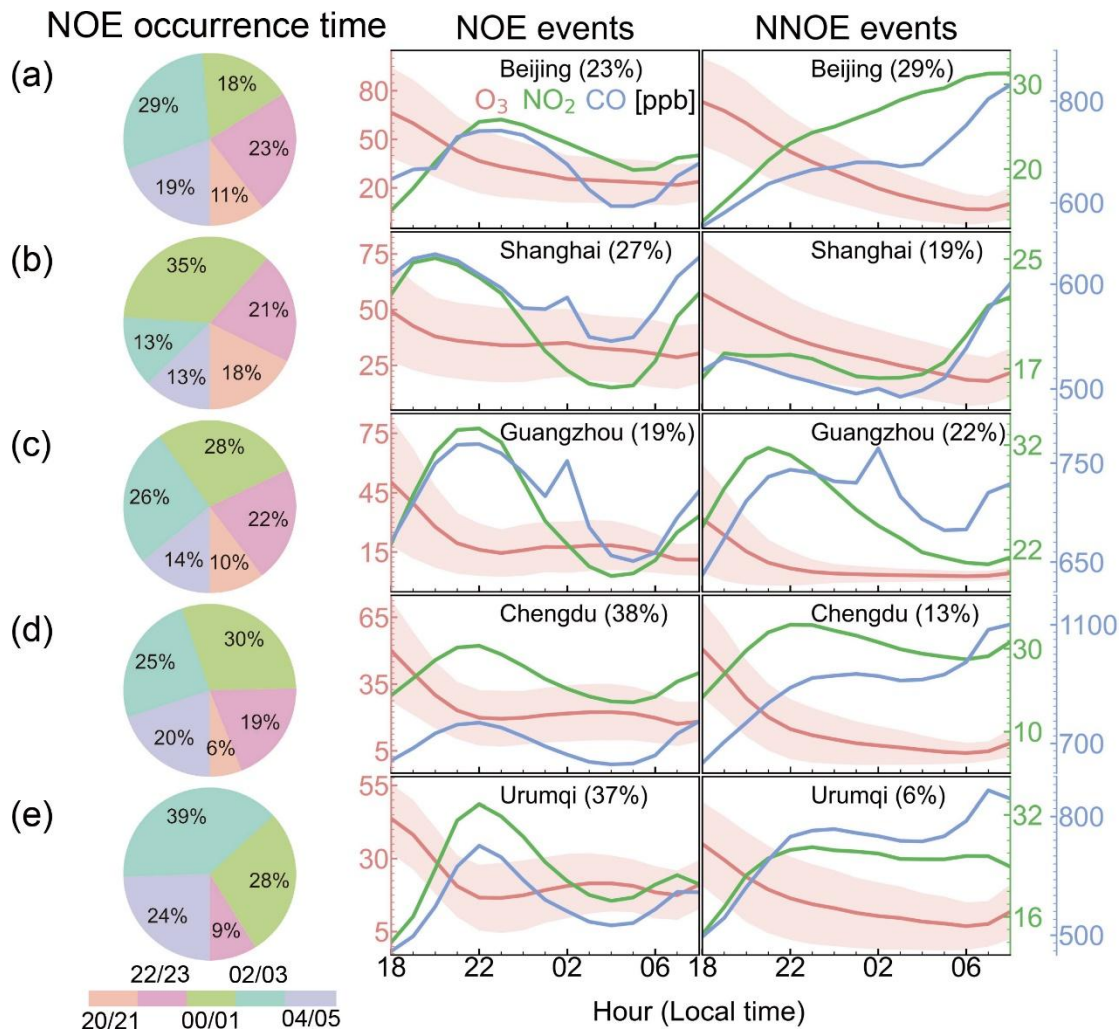
Figure 4. Comparison of the temporal variation of nocturnal air pollutants (ozone, NO₂, and CO) between the NOE and the NNOE events in the warm season in five typical cities (Beijing, Shanghai, Guangzhou, Chengdu, and Urumqi). Each city contains a number of monitoring sites, and we average the data across the sites within the city to represent ozone at the city level. The number in parentheses represents the frequency of NOE and NNOE event in the city. The estimated NOE frequency at city level based on the site-average ozone values is lower than that at site level as the occurrence time of NOE events may vary at different sites. Note that axis range for different cities varies. The pie chart shows the frequency of the occurrence time of the NOE events, defined as the time with maximum ($\Delta O_3/\Delta t$) in each NOE event.

28
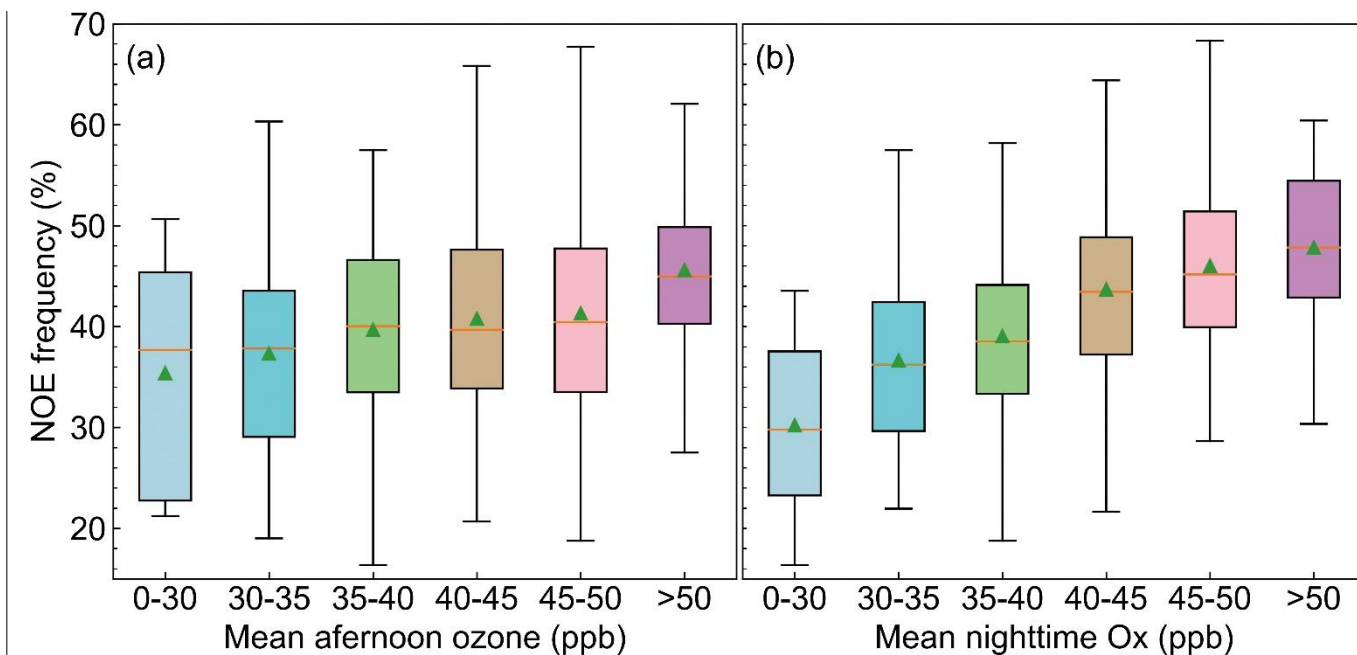
Figure 5. The relationship between NOE frequencies and afternoon ozone (a) and nighttime O_x (b) at 814 Chinese sites. The colored box-and-whisker plots (5th, 25th, 50th, 75th, and 95th percentiles, and mean values denoted as triangles) show NOE frequencies at different concentrations.

705

(a) Trends of U*, NOE vs NNOE events
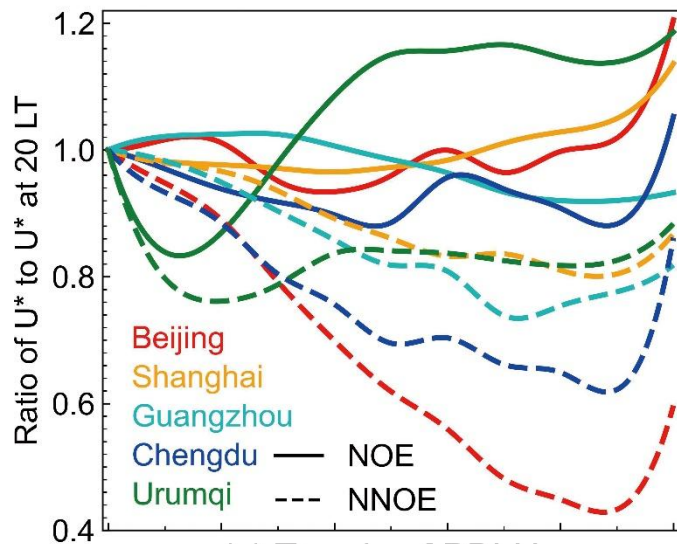
(b) Frequency of U* enhancement in NOE events

70±5%   N=814

Ratio of U* to U* at 20 LT

Beijing
Shanghai
Guangzhou
Chengdu
Urumqi
— NOE
-- NNOE
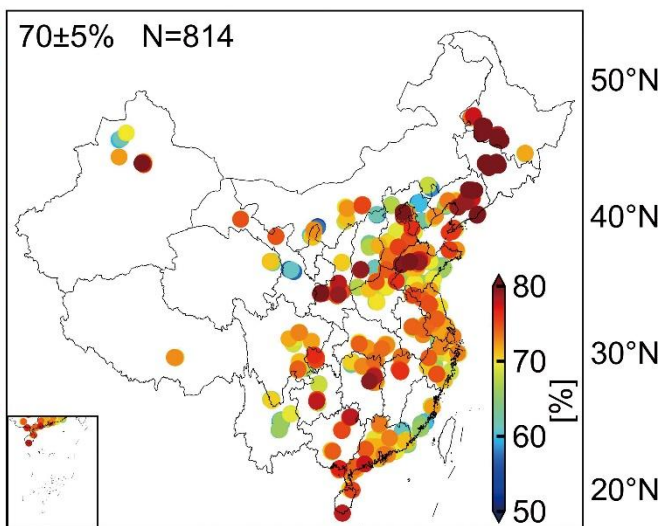
(c) Trends of PBLH, NOE vs NNOE events
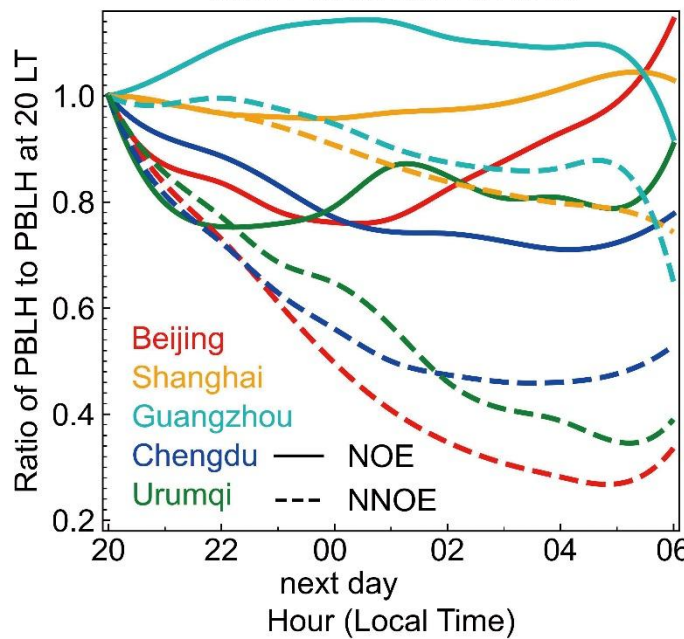
(d) Frequency of PBLH enhancement in NOE events

65±7%   N=814

Ratio of PBLH to PBLH at 20 LT

Beijing
Shanghai
Guangzhou
Chengdu
Urumqi
— NOE
-- NNOE

next day
Hour (Local Time)
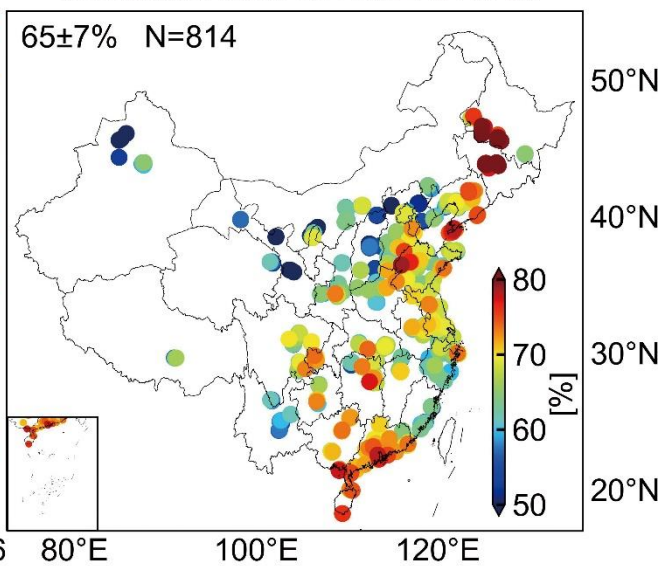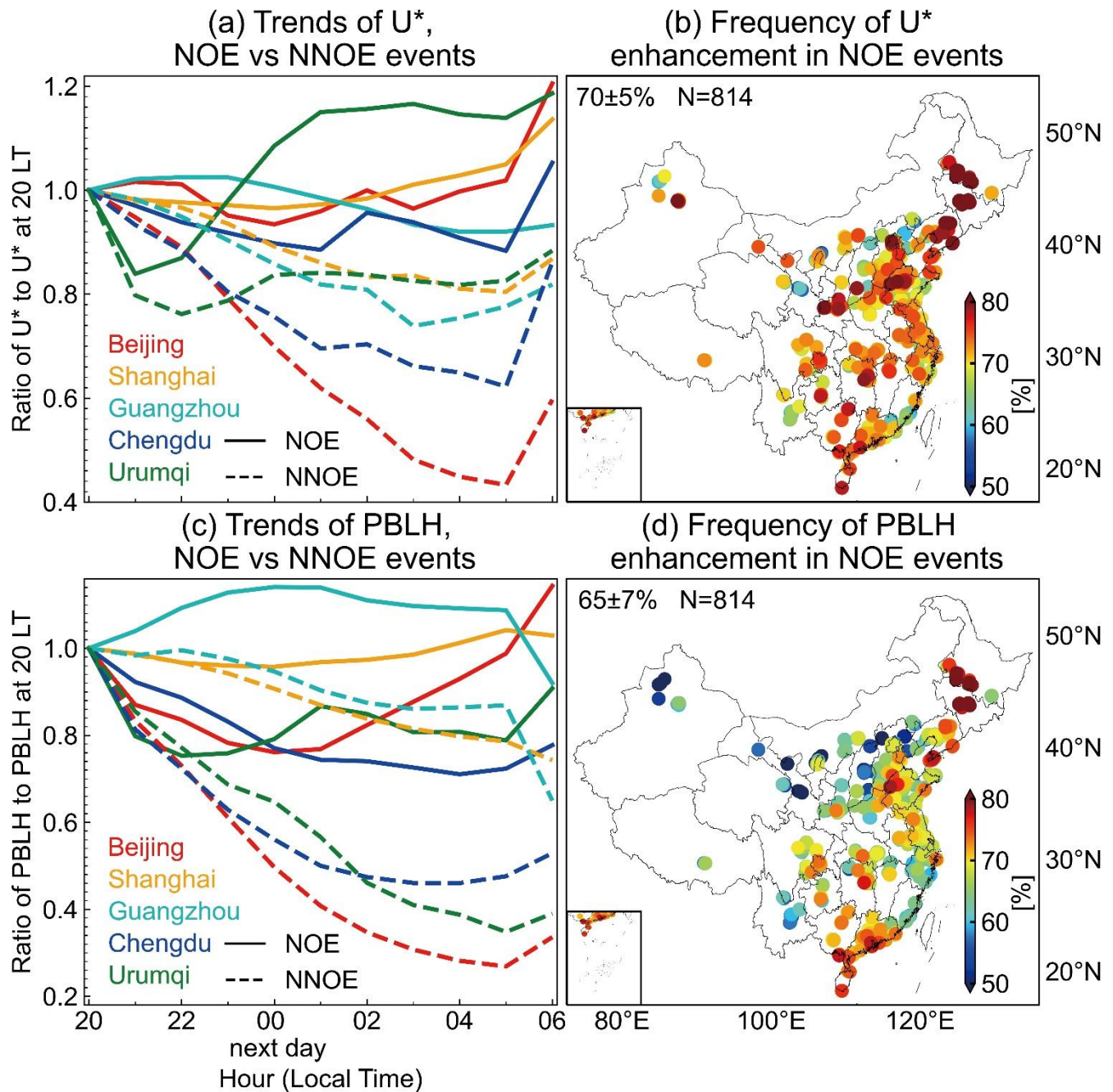
Figure 56. Increases in friction velocity (U*) and planetary boundary layer height (PBLH) in the NOE event. Panels (a) and (c) shows the nighttime evolution of the U* and PBLH, scaled by the values at 20:00 LT, averaged over all NOE and NNOE events in the five representative cities. The absolute values of U* and PBLH are shown in Figure S5. Panels (b) and (d) show the frequency of U* and PBLH increase within two hours before the occurrence time of an NOE event at individual sites. The regional mean and standard deviations among the N sites are shown inset. The U* and PBLH data are from the ERA5 dataset.
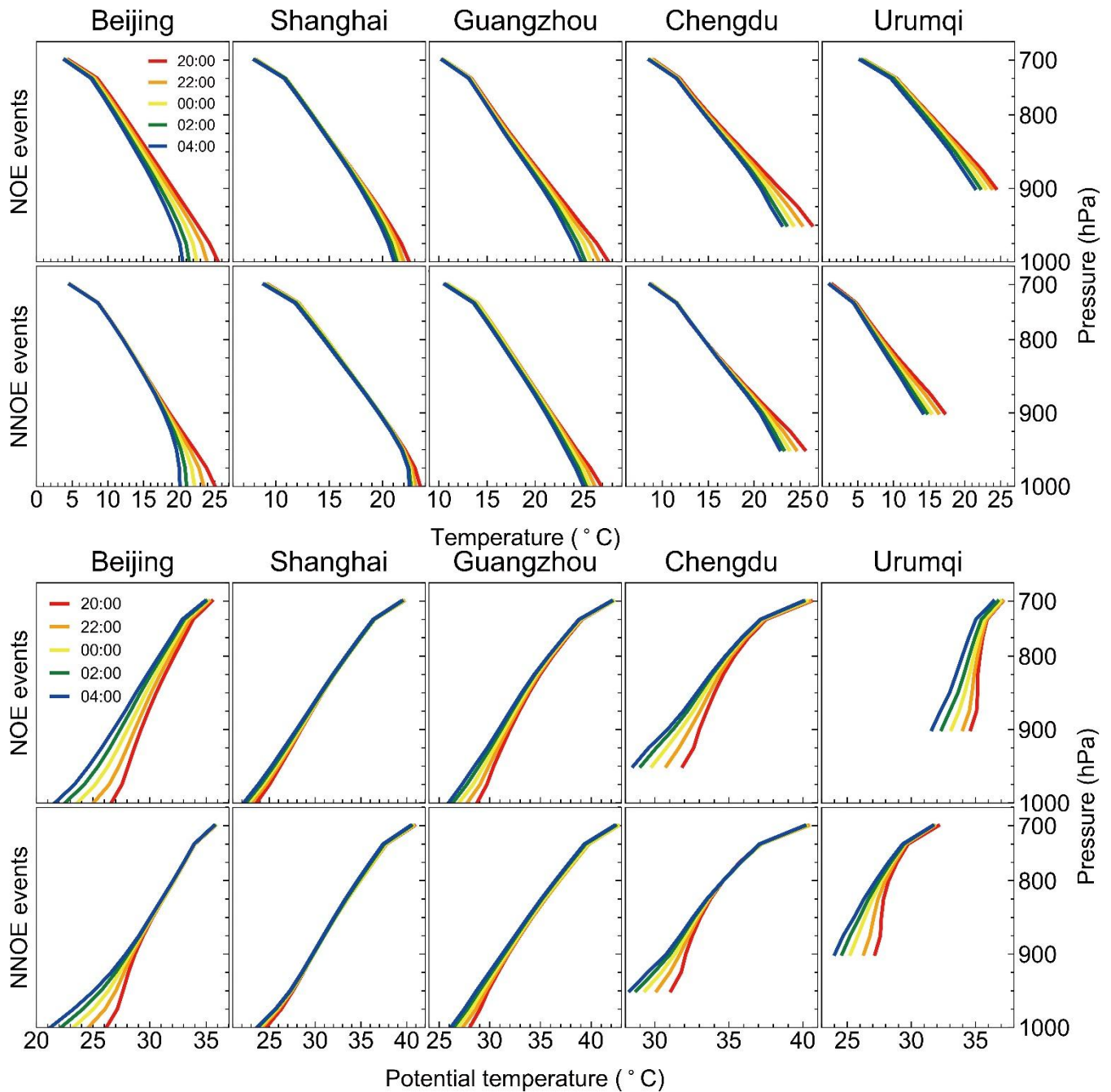
Figure 67. Comparison of vertical profiles of potential temperature at five typical cities between the NOE (the top panels) and the NNOE (the bottom panels) events. The colored lines represent potential temperature profiles at different time of the night. The temperature data are from the ERA5 dataset.
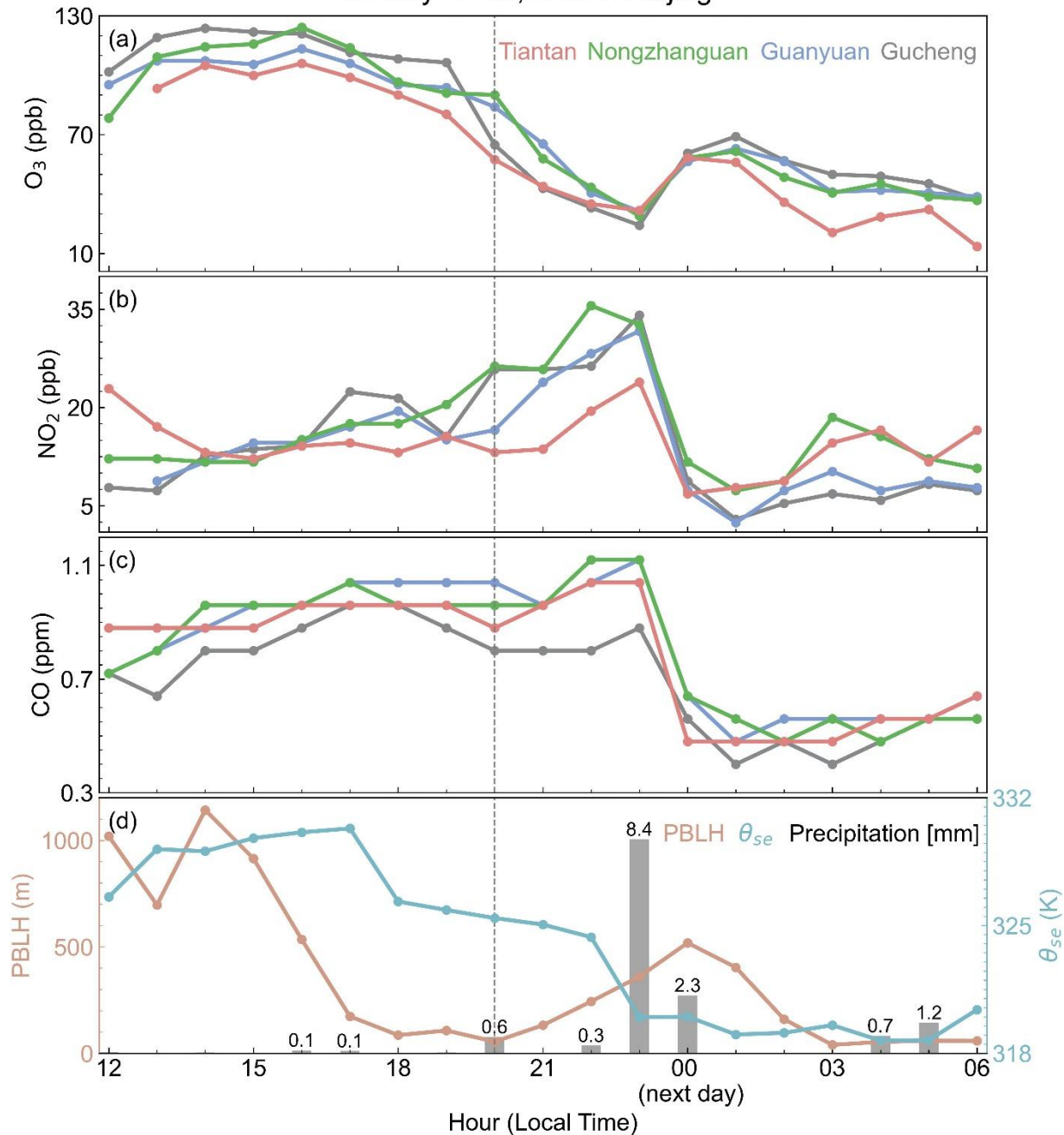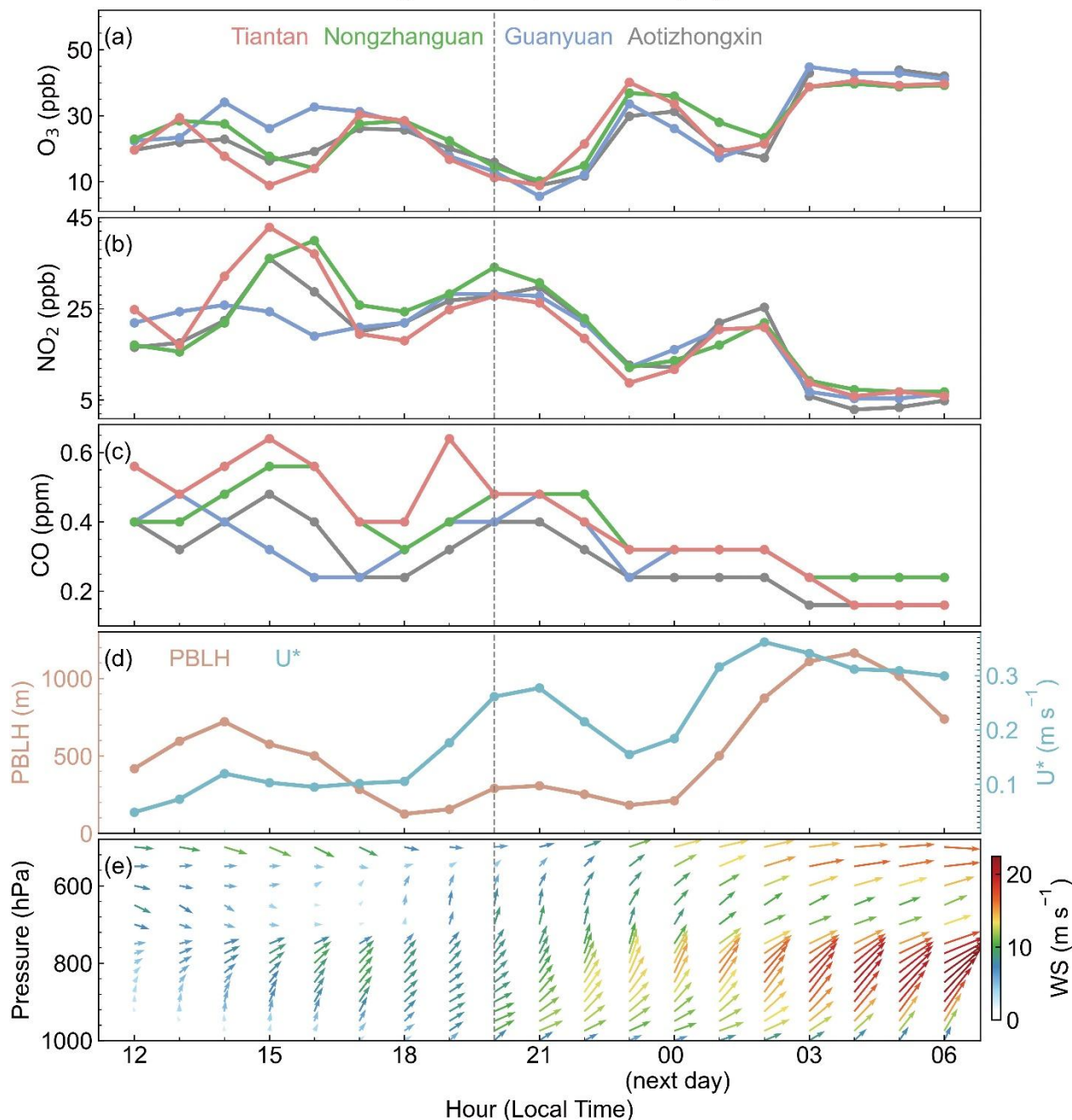
Figure 87. Hourly variations of air pollutants and meteorological parameters at four sites in a Beijing NOE event on July 29-30, 2015, induced by a convective storm. Panels (a), (b), and (c) show the evolution of ozone, NO_2, and CO, respectively. Panel (d) shows the evolution of PBLH, equivalent potential temperature (θ_{se}), and precipitation from the ERA5 dataset. The vertical dashed line marks the start of nighttime.
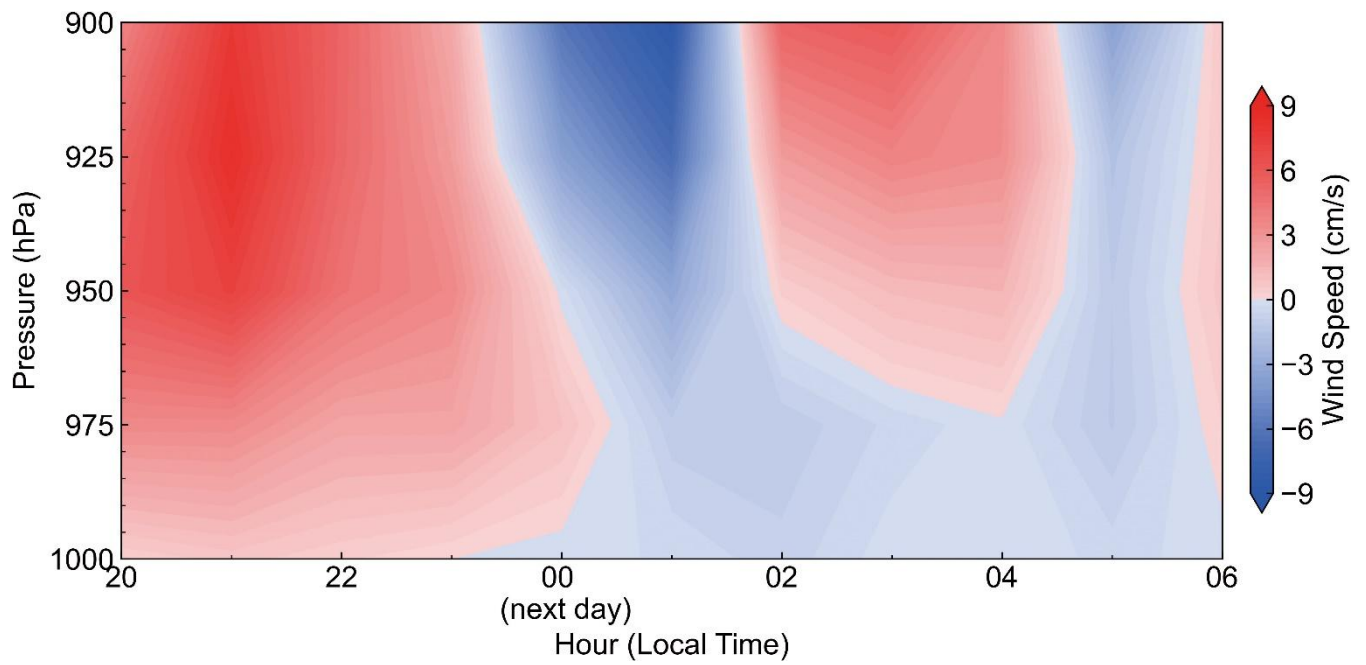
Figure 8. Evolution of vertical velocity over Beijing (116.5°E, 40°N) on July 29-30, 2015 in an NOE event.

Figure 9. Hourly variations of air pollutants and meteorological parameters at four sites in a Beijing NOE event on August 26-27, 2017, induced by low-level jets. Panels (a), (b), and (c) show the evolution of ozone, NO_2, and CO, respectively. Panel (d) shows the evolution of PBLH and frequent velocity (U*). Panel (e) shows the temporal variation of the horizontal wind profiles, with the color showing the wind speed. The vertical dashed line marks the start of nighttime.
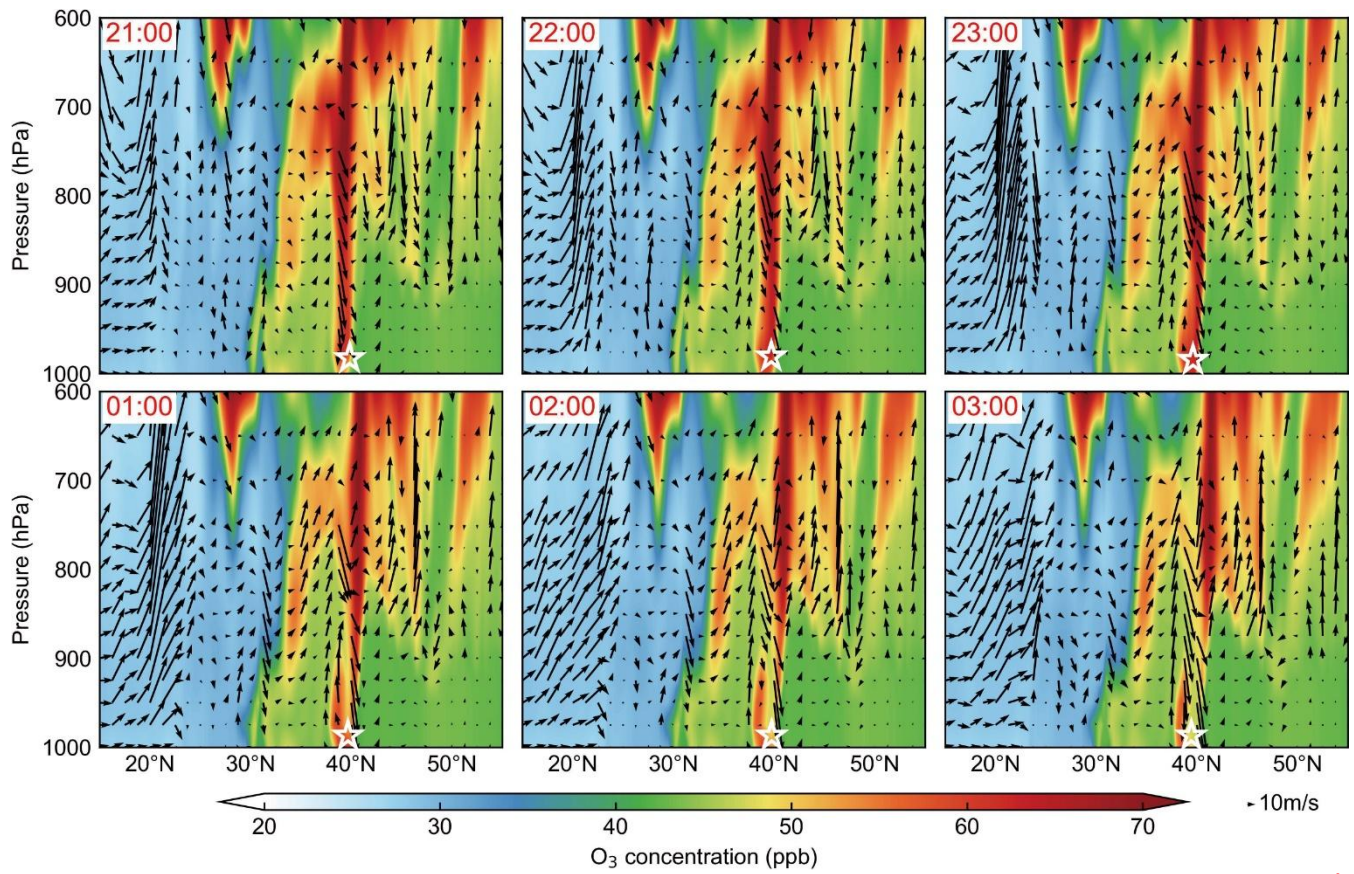
Figure 10. Latitude-altitude cross-section of ozone (shaded) and wind fields of meridional (south-north) and vertical wind (scale by 10³) (arrows) at the longitude of 116.5°E in a Beijing NOE event on August 26-27, 2017. The star marks the location of Beijing.
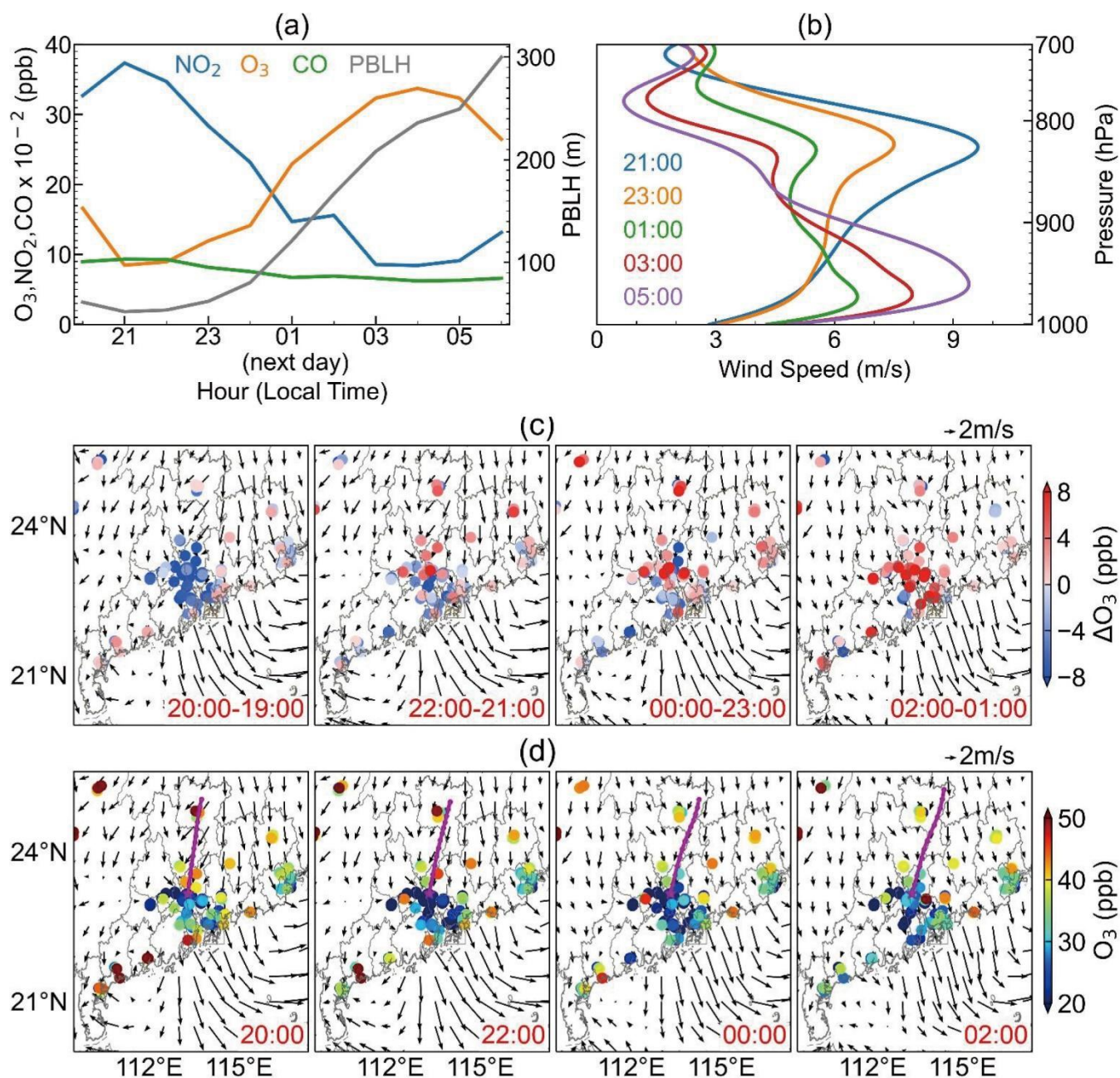
Figure 1~~1~~0. An NOE event in Guangzhou on September 21-22, 2014. Panel (a) shows the hourly variations of nocturnal ozone, NO₂, and PBLH. Panel (b) shows the evolution of vertical profiles of wind speed. Panel (c) shows the 10 m wind fields and changes in ozone relative to the previous hour. Panel (d) shows the 10 m wind fields and hourly ozone concentration. The purple line is the 12-h backward trajectories of air mass calculated using the HYSPLIT model.

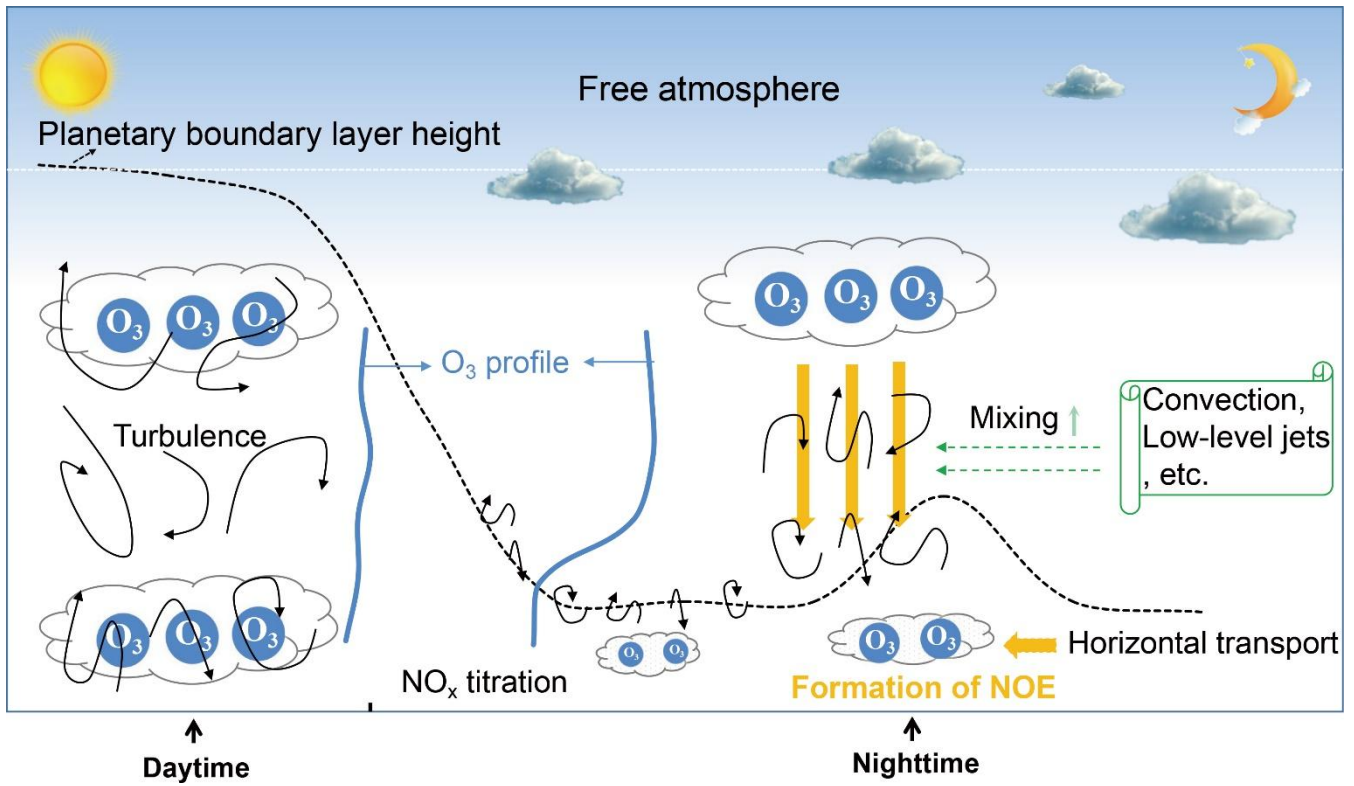**Figure 112.** Conceptual model of high frequency of NOE events over China.